Under-ice and open-water ecosystem metabolism in temperate water bodies

R.L. North[1], J. J. Venkiteswaran[2], G. Silsbe[3], J.W. Harrison[4], J.J. Hudson[5], R.E.H Smith[6], P.J. Dillon[7], P. Pernica[8], S.J. Guildford[9], M. Kehoe[8,10], H.M. Baulch[8]

[1]School of Natural Resources, University of Missouri, 303L Anheuser-Busch Natural Resources Building, Columbia, MO, 65211-7220, ORCID 0000-0003-3762-5939
[2]Department of Geography and Environmental Studies, Wilfrid Laurier University, 75 University Avenue West, Waterloo ON N2L 3C5, Canada, ORCID 0000-0002-6574-7071
[3]Horn Point Laboratory, University of Maryland Center for Environmental Science, Cambridge, MD, United States, ORCID 0000-0003-2673-1162
[4]Hutchinson Environmental Sciences Ltd., 1-5 Chancery Lane, Bracebridge, ON, P1L 2E3, Canada, ORCID 0000-0002-6024-7166
[5] Emeritus, Department of Biology, University of Saskatchewan, Saskatoon, Saskatchewan, Canada, ORCID 0000-0002-0256-3240
[6]Emeritus, Department of Biology, University of Waterloo, Waterloo, Ontario, Canada
[7]Emeritus, School of the Environment and Chemistry, Trent University, Peterborough, Ontario, Canada
[8]School of Environment and Sustainability, University of Saskatchewan, Saskatoon, Saskatchewan, Canada, Baulch: ORCID 0000-0001-9018-4998, Kehoe: ORCID 0000-0002-5281-5821
[9]Emeritus, Large Lakes Observatory University of Minnesota-Duluth, Duluth, Minnesota USA, ORCID 0000-0003-0466-2872
[10]Current affiliation: Centre for Applied Research, Innovation and Entrepreneurship, Lethbridge College, Lethbridge, Alberta, Canada

This paper is a non-peer reviewed preprint submitted to EarthArXiv. This manuscript has been submitted to the Journal of Geophysical Research: Biogeosciences for peer review. Subsequent versions of this manuscript may have slightly different content. If accepted, the final version of the manuscript will be available via the "Peer-reviewed Publication DOI" link on the right-hand side of this webpage. Please feel free to contact the corresponding author.

Twitter handle: @RebeccaNorth2

Key Points:

- This is the first-ever application of the stable isotope and fluorometric approaches to the estimation of under-ice production rates
- Year-round P:R ratios are close to unity, with autotrophy dominating in the open-water season and heterotrophy under ice
- This work serves to augment our understanding of lake ecosystem metabolism

Abstract

Winter, historically a largely un-monitored season, is influential and changing. There is evidence of the importance of under-ice phytoplankton in temperate lakes, but it is currently unknown if high winter phytoplankton biomass translates to high productivity and what influence it has on year-round lake metabolism. Winters are getting shorter, but our ability to forecast change is hindered by our limited understanding of under-ice processes. Here, we compare under-ice and open-water rates of areal gross production (AGP) and areal respiration (AR) from 3 Canadian reservoirs and one large lake using oxygen (O_2) $\delta^{18}O$-O_2 models and fluorometry. During the open-water season, AGP was 5× greater than under-ice rates, with AR rates 8× higher than measured during winter. Open-water samples indicated autotrophy (P:R= 1.10) with heterotrophy dominant under ice (P:R= 0.67). Consistent with current assumptions, the cold under-ice environment is associated with low primary productivity. Our results challenge the assumption that mean water column irradiance is lowest during the winter in dimictic water bodies; we find similar light conditions during the open-water season. Winter mean light is regulated by snow thickness; upon manual snow removal, we observe a 67 % increase in under-ice mean water column irradiance. The first-ever under-ice application of the $\delta^{18}O_2$-method indicated that AGP responded to improvements in light. This study reveals further insights into the importance of under-ice metabolism on year-round processes in a changing climate.

Plain Language Summary

Our current understanding of lake primary productivity and metabolism is based primarily on research conducted during the open-water season. Our ability to forecast climate change impacts

62 is hindered by our limited understanding of what happens under the ice. Our results challenge the
63 assumption that the light climate is lower during the winter in dimictic water bodies and
64 highlights the important role of changing light conditions on winter phytoplankton populations.
65 This work examines the relationship between winter phytoplankton biomass and productivity
66 with implications for year-round lake metabolism and carbon cycling. The paucity of year-round
67 rates makes it difficult to conclude whether "most" lakes are net autotrophic or net heterotrophic.
68 We found stochastic and brief pulses of both under-ice phytoplankton biomass and productivity
69 that would not be captured in typical monthly monitoring programs but should be considered by
70 all temperate aquatic ecosystem researchers.

1 Introduction

Emerging research in winter limnology has a common message- winter should not be ignored (Cavaliere & Baulch, 2018; Denfeld et al., 2018; Hampton et al., 2014, 2015, 2017; Katz et al., 2015; Powers et al., 2017). Its importance to structuring ecosystems differs from summer, but can be similarly influential. Winter biogeochemical research is receiving increased attention (Cavaliere & Baulch, 2018; Ducharme-Riel et al., 2015; Finlay et al., 2019; Powers et al., 2017), and changes in underwater light climate have been linked to phytoplankton dynamics (Butts & Carrick, 2017; Cavaliere & Baulch, 2020; Hampton et al., 2017; Pernica et al., 2017; Suarez et al., 2019). The impact of changing winter light climates on primary productivity, however, is still relatively unexplored (but see Howard et al., 2024) with the exception of manipulated systems (Garcia et al., 2019; Hrycik & Stockwell, 2020).

Climate-induced reductions in lake ice cover will result in shorter winters (Sharma et al., 2019). Understanding winter dynamics may be important for predicting future changes in year-round lake metabolism and ecosystem function. Under-ice, the only substantive input of oxygen (O_2) is via primary production; thus, the balance between production (P) and respiration (R) is critical to preventing winterkill and maintaining aerobic biogeochemical cycles.

Paleolimnological research has shown that fossil pigments (proxies for phytoplankton) have increased in some temperate lakes, coincident with earlier ice-out (Ewing et al., 2020). Under-ice phytoplankton blooms are increasingly reported (Reinl et al., 2023); in Lake Erie, the spring bloom is most prominent under ice (Twiss et al., 2012). Under-ice blooms were also observed in a Canadian reservoir, with Chlorophyll *a* (Chl *a*) concentrations exceeding annual mean values 15 % of times measured (Cavaliere & Baulch, 2020). A long-term study in a dimictic lake reported higher winter phytoplankton biomass during mild winters (Adrian et al.,

1995). Following mild winters, the maximum open water season biomass occurred one month earlier than normal and was dominated by cyanobacteria (Adrian et al., 1995, 1999). Seasonal shifts in phytoplankton biomass and composition have significant implications for food webs, fish habitat, biogeochemical cycling, and dead zones. It is important to understand if winter blooms translate to high primary productivity and what influence they have on year-round ecosystem metabolism.

The current metabolic paradigm considers lakes to be net heterotrophic (Del Giorgio & Peters, 1994; Hanson et al., 2003; Idrizaj et al., 2016) and thus net ecosystem producers of carbon dioxide (CO_2) and consumers of organic matter and O_2. This understanding, however, is based on metabolic rates that are measured during the open-water season in temperate water bodies. Studies with a wider seasonal scale are raising the possibility of aquatic systems being net autotrophic (Baehr & DeGrandpre, 2004; Bocaniov & Smith, 2009; Depew et al., 2006), suggesting that infrequent sampling might miss pulses of high primary production during the winter and shoulder (spring and autumn) seasons and underestimate the P:R ratio. Winter-only metabolism estimates indicate heterotrophy (Brentrup et al., 2021; Dokulil et al., 2014; Gammons et al., 2014; Obertegger et al., 2017; Rabaey et al., 2021), resulting in year-round P:R ratios less than one (Brentrup et al., 2021; Finlay et al., 2019; Howard et al., 2024; Wassenaar, 2012).

Given our current understanding of lake primary productivity and metabolism in temperate lakes is largely based on research conducted during the open-water season, our ability to forecast change is hindered by our limited understanding of what happens under the ice and what will happen under a scenario of no ice cover. Here, we report absolute rates of areal gross production (AGP) and areal respiration (AR) under ice cover over the course of 2 winters in 3

Canadian reservoirs and one large lake, representing a gradient in snow cover and morphometry, and compare estimates with open-water rates. We address the following specific questions:

1) How do under-ice rates of productivity and respiration compare with open-water rates?

2) What are the environmental drivers of under-ice productivity and respiration?

We measured under-ice community metabolism by 2 different methods. These include AGP derived from fluorometric measurements and $\delta^{18}O$-O_2-derived rates of AGP and AR. This is the first-ever application of both the $\delta^{18}O$-O_2 and fluorometric approaches to quantifying absolute under-ice primary production.

2 Materials and Methods

2.1 Study site descriptions

This study was conducted on 3 mesotrophic reservoirs in southern Saskatchewan (SK; Blackstrap, Broderick, Diefenbaker) and one oligo-mesotrophic large lake in southern Ontario (ON; Lake Simcoe; Fig. 1), Canada. All 4 water bodies are dimictic and represent a gradient in size, depth, and snow cover (Table 1). Lake Simcoe is a large (surface area = 722 km^2, mean depth = 16 m, maximum depth = 42 m; North et al., 2013), windswept lake that provides a contrast to the smaller SK reservoirs.

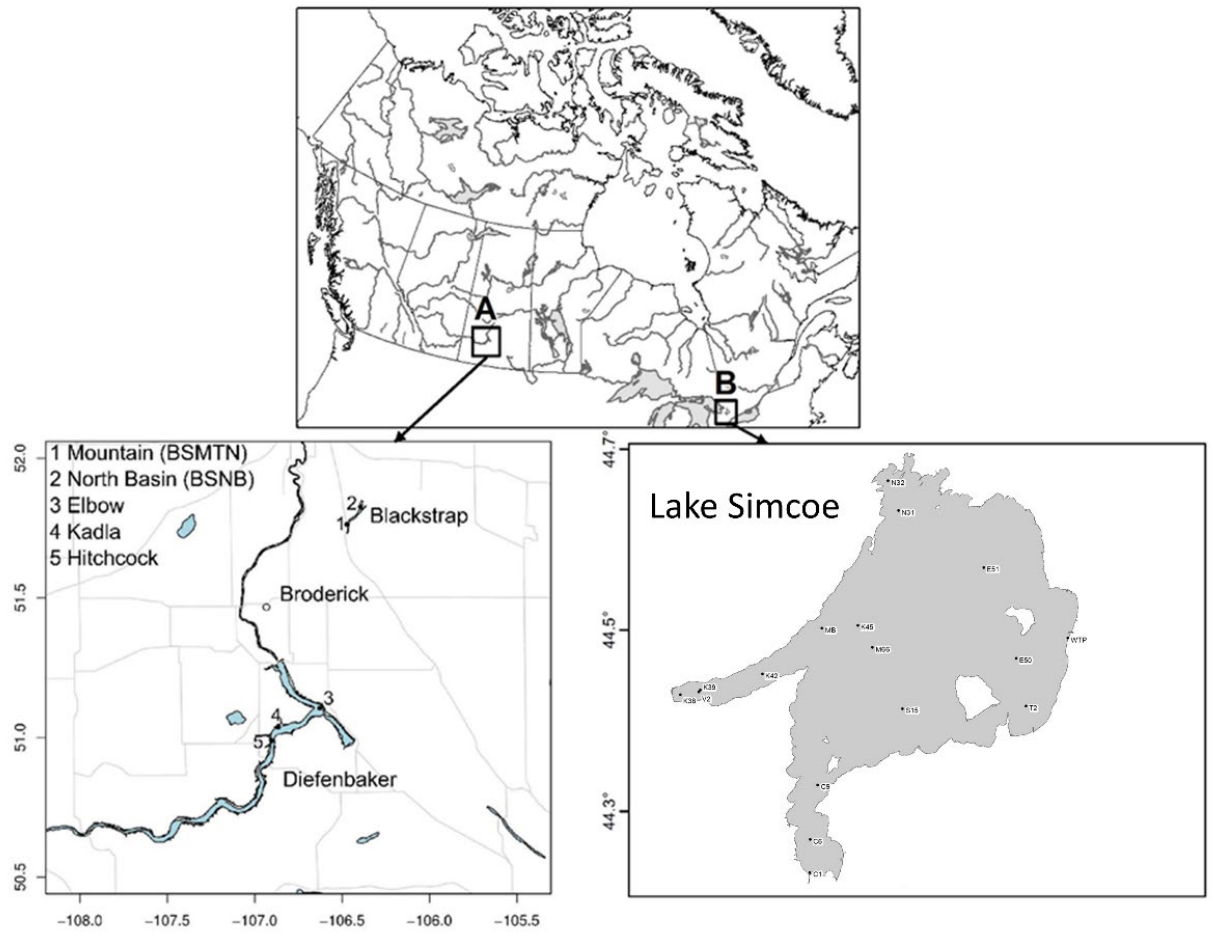

Figure 1. Map of Canadian water bodies and associated stations. a) Locations of the 3 Saskatchewan reservoirs with all sampling stations labelled: Blackstrap (1, 2), Broderick, and Diefenbaker (3, 4, 5). b) Lake Simcoe, Ontario, with all 17 stations labelled including the Beaverton water treatment plant (WTP) intake pipe.

Table 1. Physical, chemical, and biological parameters measured during the open-water and ice-covered seasons, differentiated by water body. Shown are the arithmetic mean and range (minimum, maximum) of *n* samples. Two stations were sampled on Blackstrap reservoir, one on Broderick reservoir, 3 on Diefenbaker reservoir, and 17 on Lake Simcoe (Fig. 1). NA, Not Applicable; Z, depth; PAR, Photosynthetically Active Radiation; K_d, vertical attenuation coefficient; TP, Total Phosphorus; TDP, Total Dissolved Phosphorus; DRP, Dissolved Reactive Phosphorus; TDN, Total Dissolved Nitrogen; PN, Particulate Nitrogen; NH_4^+, ammonium; NO_3^-, nitrate; Chl *a*, Chlorophyll *a*; POC, Particulate Organic Carbon; Phyto, Phytoplankton; E_k, light saturation parameter; $rETR_{max}$, maximum relative electron transport rate through PSII; α, light limited slope of the P-E curve; ANP, Areal Net Productivity; AGP, Areal Gross Productivity; AR, Areal Respiration; $\bar{E}_{24}$, mean daily mixed layer irradiance. S+I+W K_d values account for water (W), ice (I), and snow (S) attenuation, S+I K_d values account for ice and snow attenuation.

Parameter	Blackstrap Open-water (n =2)	Blackstrap Under-ice (n =9)	Broderick Open-water (n =1)	Broderick Under-ice (n =5)	Diefenbaker Open-water (n =13)	Diefenbaker Under-ice (n =9)	Simcoe Open-water (n =88)	Simcoe Under-ice (n =23)
Physical								
Z_{mix} (m)	6.8 (6.5, 7.0)	0.2 (NA, 1.0)	5.0	NA	18.0 (7.0, 37.1)	1.5 (NA, 4.5)	13.2 (2.0, 37.9)	1.1 (NA, 3.5)
Z_{snow} (cm)	NA	13.3 (0.1, 26.8)	NA	11.9 (0.7, 19.0)	NA	12.4 (1.7, 21.3)	NA	7.0 (0.1, 22.9)
Z_{ice} (cm)	NA	82.9 (58.8, 98.2)	NA	76.0 (49.3, 92.7)	NA	70.1 (57.7, 85.3)	NA	35.5 (25.4, 45.7)
$Z_{white\ ice}$ (cm)	NA	7.6 (2.7, 25.0)	NA	7.8 (5.2, 11.5)	NA	3.4 (0.0, 9.7)	NA	16.1 (10.2, 20.3)
$Z_{black\ ice}$ (cm)	NA	74.7 (54.0, 95.0)	NA	68.2 (44.1, 87.3)	NA	66.7 (56.7, 82.2)	NA	24.6 (22.9, 25.4)
Albedo	NA	1.9 (1.6, 2.3)	NA	1.8 (1.4, 2.1)	NA	1.8 (1.6, 2.1)	NA	1.1 (1.0, 1.1)
Surface PAR ($\mu mol\ m^{-2}\ s^{-1}$)	1090.2 (966.0, 1214.3)	43.7 (3.3, 262.2)	432.9	12.4 (2.3, 37.5)	1297.3 (884.9, 1760.9)	100.2 (5.7, 480.6)	862.8 (143.9, 2010.0)	157.8 (4.6, 1276.5)
Water K_d (m^{-1})	0.8 (0.7, 0.8)	0.6 (0.4, 1.1)	1.0	0.4 (0.2, 0.7)	0.7 (0.4, 1.2)	0.6 (0.4, 0.8)	0.3 (0.2, 0.5)	0.3 (0.1, 0.5)
S+I+W K_d (m^{-1})	NA	4.3 (0.6, 5.5)	NA	5.1 (3.3, 7.0)	NA	3.7	NA	NA
S+I K_d (m^{-1})	NA	3.7 (0.2, 5.0)	NA	4.7 (2.5, 6.7)	NA	3.0	NA	NA
PAR transmission (%)	NA	8.7 (1.2, 24.3)	NA	2.5 (0.9, 5.8)	NA	20.3 (0.7, 79.5)	NA	23.5 (0.9, 89.6)
$\bar{E}_{24}$ ($\mu mol\ m^{-2}\ s^{-1}$)	94.5 (90.4, 98.5)	22.1 (3.7, 68.3)	89.5	17.2 (2.3, 37.5)	43.5 (19.0, 78.7)	40.9 (0.5, 223.0)	31.0 (7.4, 74.2)	90.7 (6.7, 555.6)
Chemical								
TP ($\mu mol\ L^{-1}$)	1.32 (1.10, 1.53)	1.70 (1.40, 1.90)	0.57	0.64 (0.53, 0.74)	0.51 (0.25, 0.89)	0.36 (0.17, 0.64)	0.28 (0.16, 0.48)	0.28 (0.22, 0.52)
TDP ($\mu mol\ L^{-1}$)	0.73 (0.62, 0.85)	1.50 (1.10, 1.70)	0.29	0.47 (0.28, 0.57)	0.20 (0.14, 0.57)	0.14 (0.09, 0.19)	0.14 (0.06, 0.30)	0.19 (0.11, 0.28)
DRP ($\mu mol\ L^{-1}$)	0.08 (0.07, 0.09)	0.80 (0.40, 1.00)	0.03	0.23 (0.07, 0.38)	0.04 (0.02, 0.09)	0.05 (0.03, 0.12)	0.01 (0.01, 0.24)	0.01

TDN ($\mu mol\ L^{-1}$)	9.1 (8.2, 9.9)	27.5 (12.4, 34.2)	4.3	24.3 (10.5, 48.9)	40.6 (28.7, 60.1)	12.0 (9.8, 18.0)	3.5 (1.0, 12.9)	4.0 (0.6, 14.8)
PN ($\mu mol\ L^{-1}$)	NA	1.0 (0.6, 1.2)	NA	1.8 (1.0, 3.2)	1.7 (0.1, 8.8)	3.2 (1.3, 8.4)	0.1 (0.1, 0.8)	0.2 (0.1, 0.6)
NH_4^+ ($\mu mol\ L^{-1}$)	0.8 (0.3, 1.3)	14.1 (6.4, 23.8)	0.2	6.2 (0.2, 20.5)	0.2 (0.1, 0.9)	0.5 (0.2, 0.8)	0.1 (0.1, 0.3)	0.1 (0.1, 0.2)
NO_3^- ($\mu mol\ L^{-1}$)	8.3 (7.9, 8.6)	13.4 (4.5, 20.5)	4.2	18.1 (10.4, 28.4)	31.0 (18.2, 41.9)	12.1 (7.3, 23.2)	0.2 (0.1, 0.7)	0.2 (0.1, 1.0)
Biological								
Chl *a* ($\mu g\ L^{-1}$)	8.4 (6.1, 10.6)	3.1 (0.1, 27.8)	3.8	1.4 (0.1, 2.9)	3.3 (1.0, 8.7)	2.1 (0.7, 5.6)	1.7 (0.1, 6.5)	3.2 (0.3, 13.1)
POC ($\mu mol\ L^{-1}$)	NA	93.5 (69.1, 114.8)	NA	128.3 (64.2, 210.1)	29.9 (9.8, 89.5)	190.1 (88.9, 412.1)	18.1 (5.2, 37.5)	10.7 (0.4, 24.5)
Phyto biomass ($mg\ m^{-3}$)	567.52 (252.93, 882.12)	53.92 (35.14, 72.86)	328.59	381.67 (6.98, 1390.47)	260.29 (216.48, 317.01)	1372.61 (281.90, 6407.77)	NA	NA
PN:PP (molar)	NA	5.8 (3.7, 13.9)	NA	10.7 (5.9, 13.0)	3.4 (0.6, 14.8)	12.8 (5.9, 18.4)	1.3 (0.1, 10.3)	1.8 (0.2. 5.3)
$\bar{E}_{24}$:E_k	NA	0.1 (0.0, 0.2)	0.3	0.1 (0.0, 0.4)	0.1 (0.0, 0.2)	0.2 (0.0, 1.3)	0.2 (0.0, 0.7)	1.4 (0.1, 10.4)
E_k ($\mu mol\ m^{-2}\ s^{-1}$)	NA	231.8 (100.0, 332.6)	333.2	308.1 (96.0, 451.1)	412.7 (340.6, 495.2)	230.3 (118.0, 464.2)	142.2 (32.1, 370.2)	78.7 (2.7, 233.3)
$rETR_{max}$ (photons reemitted absorbed^{-1})	NA	47.9 (1.2, 145.0)	189.9	32.9 (9.1, 58.3)	220.9 (152.8, 263.9)	53.7 (13.7, 101.3)	70.6 (13.3, 176.1)	38.2 (1.0, 62.5)
α	NA	0.82 (0.64, 1.00)	0.57	0.60 (0.30, 0.70)	0.53 (0.45, 0.59)	0.57 (0.14, 1.00)	0.51 (0.19, 0.80)	0.67 (0.25, 4.07)
AR-$\delta^{18}O$ ($mmol\ O_2\ m^{-2}\ day^{-1}$)	96.3 (80.1, 112.5)	4.8 (0.0, 24.3)	62.6	11.7 (3.1, 33.0)	43.2 (37.7, 53.3)	0.5 (0.3, 0.9)	29.0 (8.5, 66.2)	0.7 (0.3, 1.7)
ANP- $\delta^{18}O$ ($mmol\ O_2\ m^{-2}\ day^{-1}$)	20.0 (17.9, 22.1)	-5.2 (-24.3, -1.8)	10.9	-12.9 (-33.0, -4.6)	6.5 (2.5, 9.0)	0.0 (-0.4, 0.5)	2.9 (-10.5, 19.8)	0.1 (0.0, 0.2)
AGP:AR-$\delta^{18}O$	1.2	0.0 (0.0, 0.3)	1.2	0.0 (0.0, 0.1)	1.1 (1.1, 1.2)	1.2 (0.6, 2.7)	1.1 (0.8, 1.7)	1.2 (1.1, 1.4)

148

149 Lake Simcoe was sampled year-round in 2010–2011 and the SK reservoirs in 2013–2014.
150 Seventeen stations were sampled intermittently on Lake Simcoe; the most frequently sampled
151 stations were sampled 3 times over the 6-week winter of 2011. The Lake Simcoe stations
152 represented a gradient between nearshore (minimum station depth, 2 m) and offshore regions
153 (maximum station depth, 42 m; Fig. 1). See North et al (2013) for a bathymetric map. On Lake
154 Simcoe, the Beaverton water treatment plant (WTP) intake pipe was sampled from January to
155 July, 2011 to supplement sampling during unstable ice cover (Kim et al., 2015; Quinn et al.,
156 2013). Ice-on occurred on January 6, 2011 on Lake Simcoe and November 10, 2012 and
157 November 6, 2013 on the SK reservoirs.
158 Lake Diefenbaker, SK is a run-of-the-river reservoir along the South Saskatchewan
159 River, with an area of 394 km^2, a mean depth of 22 m, and a maximum depth of 59 m. Three
160 stations were sampled on Lake Diefenbaker representing the main channel (Hitchcock,
161 maximum depth 25 m), an embayment (Kadla, maximum depth 11.8 m), and the deeper
162 lacustrine region (Elbow, maximum depth 31.8 m; North et al., 2015; Fig. 1). See Sadeghian et al
163 (2015) for a bathymetric map. Originating from the Qu'Appelle Dam on Lake Diefenbaker,
164 gravity-fed canals transport water downstream through Broderick and Blackstrap reservoirs.
165 Broderick reservoir has a surface area of 4 km^2, with a mean depth of 6 m and a maximum depth
166 of 7 m; one station represents this reservoir. Blackstrap reservoir has a surface area of 12 km^2,
167 with a mean depth of 5 m and maximum depth of 9 m. Two stations were sampled (Fig. 1), one
168 in the north basin (Blackstrap North Basin [BSNB], depth 7.5 m) and the other in the south basin
169 (Blackstrap Mountain [BSMTN], depth 8 m; Fig. 1).
170 2.2 Field sampling
171 Sampling was conducted from a boat during the open-water season. During winter, we accessed

the same stations by snowmobile and sampled through holes in the ice (Block et al., 2019). Water was collected from discrete depths (0–2 m; North et al., 2023) for various analyses (Table 1) and $\delta^{18}O$-O_2 stable isotope samples were collected from one to 4 depths per station, depending on water column depth and lake thermal structure that day. Sample dates can be found in North et al., (2023). Water samples were collected in acid-washed 20 L carboys, protected from exposure to direct sunlight and temperature fluctuations, and were processed the same evening. On all water bodies, a Yellow Springs Instrument sonde (model 6600 V2) was used to obtain high-resolution vertical profiles of depth, temperature (accuracy = ±0.15 °C, resolution = 0.01 °C), specific conductance (accuracy = ±0.5 %, resolution = 0.001 mS cm^{-1}), O_2 (6150 ROX optical O_2 sensor that was calibrated weekly; accuracy = ±0.1 mg L^{-1}, resolution = 0.01 mg L^{-1}) and Chl *a* (resolution = 0.1 μg L^{-1}) concentrations at each station. Open-water season epilimnion (defined by a change in water temperature of > 0.5 °C m^{-1}) and convective mixed layer thickness (Z_{mix}) were calculated from temperature profiles. We calculated site- and date- specific solar-induced under-ice convective mixed layers on all 4 water bodies defined as the region where the convective Richardson number is ≤ 1 (Pernica et al., 2017).

2.3 Physical parameters

Triplicate snow depth measurements were taken on the SK reservoirs with a metric avalanche probe (Block et al., 2019). These represented locations where snow had accumulated and where snow had been removed by wind on the ice surface. Triplicate measurements of ice thickness (Z_{ice}) were recorded using a weighted measuring tape. Black ice ($Z_{black\ ice}$; congelation ice) and white ice ($Z_{white\ ice}$; snow ice) thicknesses were differentiated visually. On Lake Simcoe, snow and ice thicknesses ($Z_{snow+ice}$) were recorded from a single hole.

On all 4 water bodies, vertical profiles (0.5 m increments) of photosynthetically active

radiation (PAR) were measured with a Li-Cor scalar (4 pi) or a cosine (2 pi) underwater quantum sensor (Model LI-193SA; Li-Cor, Lincoln, NE, USA). The linear regression of the natural logarithm of irradiance versus depth was calculated from these profiles (Kirk, 1994). To account for the additional effect of attenuation of light through snow and ice, under-ice K_d was determined based on the incident irradiance above ($\bar{E}_0^+$; albedo-corrected) and below (surface PAR) the snow-ice pack with $Z_{snow+ice}$ following the Beer-Lambert equation (K_d = - log(surface PAR / $\bar{E}_0^+$) / $Z_{snow+ice}$). PAR transmission (%) was calculated as surface PAR / $\bar{E}_0^+$. To measure underwater PAR under snow and ice, a model (model I linear regression, R^2_{adj}= 0.972, p< 0.0005, n= 19, $\log_{10}$ transformed data) was developed to convert cosine to scalar readings by multiplying by a factor of 1.85. The PAR sensor was lowered under the ice through a 20.32 cm diameter hole using an articulated arm that positioned the sensor flush with the lower ice surface at a distance 1 m from the hole (surface PAR). The integrity of the snow cover was preserved in order to represent realistic transmittance through ice and snow. Albedo was calculated as the ratio of upwelling irradiance ($\bar{E}_u$) to downwelling irradiance ($\bar{E}_d$) collected with the Licor sensor as above at a height of 1 m above the snow or ice surface (Belzile et al., 2001). We accounted for the effect of Z_{snow} on albedo with 17 PAR measurements from our SK sites in 2014 (model I linear regression, albedo= [0.017 × Z_{snow}] + 0.654, R^2_{adj}= 0.52, p= 0.001, n= 17). Incident irradiance PAR measured in air ($\bar{E}_{air}$) with a cosine sensor were also adjusted to scalar readings by applying another correction actor (model I linear regression, R^2_{adj}= 0.855, p< 0.0005, n= 16) which involved the multiplication of cosine readings by a factor of 4.25 to yield scalar $\bar{E}_{air}$. Albedo estimates were calculated for each sampling occasion and $\bar{E}_0^+$ values were corrected for derived albedo as follows: $\bar{E}_0^+$= $\bar{E}_{air}$ × (1-albedo). In 2010–2011, mean daily (24-hour) incident irradiance (daily $\bar{E}_0$) was modelled from latitude and day of year assuming 75 % of theoretical

cloud-free values (Kim et al., 2015). In 2013–2014, daily $\bar{E}_0$ was scaled to PAR using a factor of 2.047 from global radiation at a nearby meteorological station (University of Saskatchewan, Saskatoon, SK; http://www.usask.ca/weather/kfarm/data/; Dubourg et al., 2015). For AGP calculations (provided below), daily $\bar{E}_0$ was converted to incident irradiance below the snow/ice ($\bar{E}_0^-$) using the formula $\bar{E}_0^-$ = daily $\bar{E}_0 \times \exp(-K_d \times Z_{snow+ice})$. We derived mean daily mixed layer irradiance ($\bar{E}_{24}$) from water K_d, Z_{mix} (Table 1), and daily $\bar{E}_0$:

$$\bar{E}_{24} = \text{daily } \bar{E}_0 \times (1 - \exp(-1 \times K_d \times Z_{mix})) \times (K_d \times Z_{mix})^{-1} \quad (1)$$

where $\bar{E}_{24}$ describes the amount of light experienced in the convective mixed layer by suspended phytoplankton over a 24-hour period. If the convective mixed layer was absent, under-ice surface PAR was reported as $\bar{E}_{24}$.

We applied physiological light deficiency thresholds to open-water and under-ice phytoplankton communities. Light thresholds for photosynthetic activity (7.6 µmol m^{-2} s^{-1}) and biomass (20 µmol m^{-2} s^{-1}) estimated from sea-ice microalgae by Gosselin et al. (1985) were applied to our under-ice data. During the open-water season, we applied 41.7 µmol m^{-2} s^{-1} (Hecky & Guildford, 1984). We also applied the ratio of $\bar{E}_{24}/E_k$ to assess light-deficiency, where E_k is the light saturation parameter derived from fluorometric rapid light curves (RLC, described below). When $\bar{E}_{24} > E_k$, there is theoretically enough light for photosynthesis. Alternatively, when $\bar{E}_{24} < E_k$, phytoplankton may experience light-deficient conditions (Hecky & Guildford, 1984). The threshold for light limitation of photosynthesis is an $\bar{E}_{24}/E_k$ ratio of one.

2.4 Chemical parameters

Total and dissolved phosphorus (P) and nitrogen (N) forms were measured on surface (0–2 m) water samples. All dissolved nutrient forms were filtered through 0.2 µm pore size polycarbonate filters. In 2010–2011, total P (TP) and total dissolved P (TDP) were analyzed with standard

241 colorimetric methods (Ontario Ministry of the Environment (OMOE), 2007b). Dissolved reactive
242 P (DRP) was analyzed according to Stainton et al. (1977). In 2013–2014, TP, TDP, and DRP
243 were measured according to Parsons et al. (1984). Particulate P (PP) was calculated by difference
244 (TP-TDP). Total dissolved N (TDN) was measured following (Ontario Ministry of the
245 Environment (OMOE), 2008) in 2010–2011 and via second derivative spectroscopy (Bachmann
246 & Canfield, 1996; Crumpton et al., 1992) in 2013–2014. Particulate N (PN) samples were
247 filtered onto pre-combusted (450 °C for 4 h) GFF (nominal pore-size 0.7 μm) filters, which were
248 immediately dried and stored in a desiccator until analysis on a MACRO CNS analyzer
249 (Elementar, Hanau, Germany) in 2010–2011. In 2013–2014, PN samples were collected on pre-
250 combusted quartz filters (GF75, nominal pore size 0.39 μm) and analyzed via an ANCA-GSL
251 sample preparation unit and Tracer 20 mass spectrometer (Europa Scientific). Ammonium
252 (NH_4^+) samples were filtered and analyzed fluorometrically according to (Holmes et al., 1999).
253 Nitrate (NO_3^-) samples were filtered and analyzed using a standard colorimetric method (Ontario
254 Ministry of the Environment (OMOE), 2007a) in 2010–2011, and via second-derivative
255 spectroscopy (Bachmann & Canfield, 1996; Crumpton et al., 1992) in 2013–2014.

256 2.5 Biological parameters

257 Samples for Chl *a* analysis were filtered onto glass fiber filters (GFF, nominal pore-size 0.7 μm)
258 and stored in the dark at -20 °C. In 2010–2011, filters were passively extracted with 90 %
259 acetone in the freezer. A fluorometer (Turner Designs 10-AU; Turner Designs, Sunnyvale,
260 California, USA) that was calibrated yearly with pure Chl *a* was used to determine the
261 pheophytin-corrected Chl *a* concentrations (Smith et al., 2005). In 2013–2014, Chl *a* extraction
262 followed (Bergmann & Peters, 1980) and (Webb et al., 1992) with ethanol as a solvent. Samples
263 were corrected for pheophytin using a spectrophotometer (UV-4201 PC, Shimadzu).

In 2010–2011, surface water for particulate organic carbon (POC) was filtered onto pre-combusted (450 °C for 4 h) GFF (nominal pore-size 0.7 μm) filters, which were immediately dried and stored in a desiccator until analysis. The dried filters were analyzed on a MACRO CNS analyzer (Elementar, Hanau, Germany). In 2013–2014, POC samples were collected on pre-combusted quartz filters (GF75, nominal pore size 0.39 μm), dried and stored until analyzed on an ANCA-GSL sample preparation unit and Tracer 20 mass spectrometer (Europa Scientific). In all years, carbonates were removed from the POC filters by fumigation using concentrated hydrochloric acid (37 %) in a desiccator for 4 h.

Phytoplankton biomass was determined on discrete whole water samples (0–2 m) via microscopic counts conducted by Plankton R Us, Winnipeg, Manitoba (Findlay & Kling, 1998) and reported as cell wet-weight biomass. Biomass was estimated by approximating cell volume and assuming one as the cellular biomass specific gravity. A minimum of 400 – 600 phytoplankton cells were enumerated using a simple counting chamber fitted to an inverted microscope. Phytoplankton were enumerated to the species level where filaments were counted individually and colonies were partially counted.

2.6 Phytoplankton nutrient status

Phytoplankton P deficiency was assessed using the stochiometric ratio of PN:PP, which was compared to an established deficiency threshold (Healey & Hendzel, 1979; Hecky & Guildford, 1984). Ratios of PN:PP >22 indicate P deficiency.

2.7 Metabolism

Two different methods were used to measure under-ice and open-water plankton areal gross production (AGP). Fluorometry (Fluoro) via a Water-PAM fluorometer (Heinz Walz GmbH, Effeltrich Germany) was used to estimate photosynthesis-irradiance (P-E) parameters (light

saturation parameter, E_K; light-limited slope of the P-E curve, α; maximum relative electron transport rate through PSII, $rETR_{max}$) and derived AGP_F rates on all 4 water bodies. O_2 concentrations and $\delta^{18}O$-O_2 values were used to model AGP-$\delta^{18}O$ and areal respiration (AR-$\delta^{18}O$) rates on all 4 water bodies. Areal net production (ANP) rates were determined from the difference between AGP-$\delta^{18}O$ and AR-$\delta^{18}O$ (ANP-$\delta^{18}O$). The P:R metabolic ratio was also calculated from $\delta^{18}O$-O_2 (AGP:AR-$\delta^{18}O$).

A Water-PAM fluorometer controlled by WinControl software (version 3.22) was used to obtain RLCs to estimate P-E parameters and derive AGP_F rates. Prior to obtaining the RLCs, whole-water samples were dark acclimated for 30 min at 20 and 4 °C during the open-water and under-ice sampling seasons, respectively. RLC measurements were obtained in triplicate and corrected for background fluorescence with sample filtrate (0.2 µm pore size polycarbonate filter). RLCs comprised 8, 1 min intervals of increasing photon flux density (PFD; range 3–1461 µmol photon m^{-2} s^{-1}). P-E parameters (E_K, α, $rETR_{max}$= E_K × α) were estimated from each RLC by fitting the equation of Webb et al. (1974) to the Photosystem II (PSII) quantum yield (Φ_{PSII}) as a function of irradiance (Silsbe & Kromkamp, 2012; Webb et al., 1974):

$$\Phi_{PSII}(E) = \alpha \times E_K \times \left(1 - \mathrm{e}(-\mathrm{E} \times E_K)\right) \times E^{-1} \quad (2)$$

The phytoplankton pigment absorption coefficient was estimated using the quantitative filter technique (Petty et al., 2020; Silsbe et al., 2012; Tassan & Ferrari, 1995). AGP_F was calculated with the R package 'phytotools' (Silsbe & Malkin, 2015) and integrated through depth and time (Petty et al., 2020).

AGP-$\delta^{18}O$ and AR-$\delta^{18}O$ rates were calculated from the measured O_2 (via sonde) and $\delta^{18}O$-O_2 values. Samples for $\delta^{18}O$-O_2 were collected in pre-evacuated 125 mL serum bottles, capped with butyl blue stoppers, and preserved with sodium azide. Before analysis, a 5 mL

helium headspace was added to each bottle by displacing an equivalent volume of water. Headspace and dissolved phases were equilibrated by manual shaking. Analysis of a subsample of headspace was performed on a modified MicroMass IsoChrom with a 5Å molecular sieve. Precision of the analysis is 0.2 ‰. Samples for $\delta^{18}O\text{-}H_2O$ were collected in triplicate and analyzed on a Los Gatos Liquid-Water Isotope Analyzer, DLT-100. Precision of the measurement is 0.2 ‰. A 1 mL aliquot was pipetted into a 2 mL vial and sealed with TST septum with cap. Working Standards (purchased from Los Gatos) were run along with samples. Post analysis, data were screened for contamination using LWIA – Spectral Contamination Identifier (software from Los Gatos), followed by correction with LWIA Post Analysis v2.2 software. Certificate of Compliance for the instruments indicate a 0.2 ‰ for $\delta^{18}O\text{-}H_2O$ and 0.6 ‰ for $\delta^{2}H\text{-}H_2O$. Both $\delta^{18}O\text{-}O_2$ and $\delta^{18}O\text{-}H_2O$ results are reported relative to SMOW. We developed a model that extends the steady-state model based on P:R ratios (Quay et al., 1995) to absolute rates (Bocaniov et al., 2015). The deviation from equilibrium saturation conditions of both O_2 and $\delta^{18}O\text{-}O_2$ values is combined with the gas exchange coefficient and Z_{mix} to calculate metabolic rates as:

$$P = \frac{k_{O2,t}}{Z_{mix}} \times \frac{O_2 \times (b-c) - O_{2s} \times (a-c)}{d-c} \quad (3)$$

$$R = \frac{k_{O2,t}}{Z_{mix}} \times \frac{O_2(b-d) - O_{2s}(a-d)}{d-c} \quad (4)$$

where k is the gas exchange coefficient for O_2 at the field temperature (m day^{-1}), O_2 is the measured concentration (mmol m^{-3}), O_2s is the 100 % saturation concentration at the field temperature (mmol m^{-3}; Benson & Krause, 1984), and a, b, c, and d are:

$$a = \alpha_g \times \alpha_s \times R_{atm} \quad (5)$$

$$b = \alpha_g \times R_{O2} \quad (6)$$

$$c = \alpha_R \times R_{O2} \quad (7)$$

$$d = \alpha_P \times R_{H2O} \quad (8)$$

where α_g is the gas exchange fractionation factor (0.9972; Knox et al., 1992), α_s is the O_2 solubility fractionation factor (1.007; Benson et al., 1979), α_R is the respiration fractionation factor (0.985; Kiddon et al., 1993; Quay et al., 1995), α_P is the photosynthesis fractionation factor (1.000; Guy et al., 1989, 1993; Helman et al., 2005; Stevens et al., 1975), R_{atm} is the isotopic ratio of atmospheric O_2 (0.0020523 since $\delta^{18}O$-O_2 is +23.5 ‰; Kroopnick & Craig, 1972), R_{O2} is the measured isotopic ratio of O_2, and R_{H2O} is the measured isotopic ratio of H_2O. To estimate k, hourly wind speeds from the previous 7 days at nearby meteorological stations were combined with 2 common windspeed to k_{600} relationships and averaged (Cole & Caraco, 1998; Crusius & Wanninkhof, 2003). The k_{600} values were converted to the Schmidt number for O_2 at the appropriate field temperature by Schmidt number scaling:

$$Sc_{O2,T} = 1800.6 - 120.10 \times T + 3.7818 \times T^2 - 0.047608 \times T^3 \quad (9)$$

$$k_{O2,T} = k_{600} \times \left(\frac{Sc_{O2,T}}{600}\right)^{\frac{-2}{3}} \quad (10)$$

where $Sc_{O2,T}$ is the Schmidt number of O_2 at a given temperature, T (°C), and the exponent -2/3 describes the surface conditions of the water (Jähne et al., 1987).

Under-ice whole-water metabolism was estimated from changes in O_2 and $\delta^{18}O$-O_2 assuming ice cover prevents gas exchange with the atmosphere. Ice-cover dates were determined from the 4 km-resolution IMS Daily Northern Hemisphere Snow and Ice Analysis data (NSIDC: National Snow and Ice Data Center, 2008). Metabolic rates were determined by best-fit modelling of the changes in measured O_2 and $\delta^{18}O$-O_2 values since ice-on as:

$$\frac{dO_2}{dt} = P - R \quad (11)$$

$$\frac{d\delta^{18}O - O_2}{dt} = P \times R_{H2O} \times \alpha_P - R \times R_{O2} \times \alpha_R \quad (12)$$

Initial conditions for modelling assumed atmospheric equilibrium values for O_2 and $\delta^{18}O$-O_2. To assess the potential variability in rates and include measurement error, the model was run in a Monte Carlo fashion 100 times per sample (each date-site-depth combination) with randomly chosen initial metabolic rates and error on the measured field values of O_2 and $\delta^{18}O$-O_2 randomly drawn from the precision around each measurement. In this way, the rates incorporate the uncertainty associated with field measurements. Expecting under-ice metabolic rates to be no greater than maximum open-water values, initial rates were chosen at random from values between zero and the maximum measured open-water rates. Best fits were determined by minimizing the difference between measured field data and model data for both O_2 and $\delta^{18}O$-O_2 values using the *ode* function in the R package deSolve (Soetaert et al., 2010). Results are summarized as median rates with median absolute deviation as a robust measure of variability since model results were expected to be non-normally distributed. Simulations with 100 and 1000 runs per sample indicate that the difference in medians and median absolute deviation differed by less than 0.1 %. Winter rates are reported at specific depths; epilimnetic rates are from a 2 m water sample. Open-water season epilimnetic rates are reported as averages of discrete samples from above the thermocline.

2.8 Statistical analysis

All assumptions of normality were tested on data subjected to parametric analysis and transformations were applied as needed. Tests of Pearson correlation were employed to assess the relationship between snow depth, ice thicknesses, and surface PAR, as well as AGP_F, $\bar{E}_{24}$, days since ice-on, AGP-$\delta^{18}O$, and AR-$\delta^{18}O$. A 2-way Analysis of Variance (ANOVA) with season (open-water and under-ice) and water body (Blackstrap, Broderick, Diefenbaker, Simcoe) as factors was applied to compare $\bar{E}_{24}$, AGP-$\delta^{18}O$, ANP-$\delta^{18}O$, AR-$\delta^{18}O$, E_k, and $\bar{E}_{24}$:E_k; if the

differences were significant, they were followed with *post hoc* Tukey-Kramer tests. The AGP method comparison was conducted via a one-way ANOVA with method as factor. A simple linear regression analysis was used to assess photoacclimation.

3 Results

3.1 Under-ice light environment and controls on productivity

Low winter primary productivity is often attributed to low light conditions. We measured under-ice PAR on all 4 water bodies under ambient snow and ice conditions and then conducted snow removal experiments to assess the impact on PAR at the ice-water interface. The only significant predictor of under-ice PAR was snow depth (r= -0.641, p< 0.0005, n= 39). There was no relationship between under-ice PAR and total ice thickness (r= -0.153, p= 0.353, n= 39), nor white ice thickness (r= -0.02, p= 0.929, n= 22), nor black ice thickness (r= -0.236, p= 0.278, n= 23). Under ice PAR values can be assessed for light deficiency for phytoplankton according to a light intensity threshold for biomass accrual (<20 μmol m^{-2} s^{-1}; Gosselin et al., 1985) and a lower threshold for photosynthesis (<7.6 μmol m^{-2} s^{-1}; Gosselin et al., 1985) as measured in sea ice phytoplankton. Under ambient snow cover, under-ice PAR was deficient for biomass accrual 51 % of the 39 times measured and 26 % of the time it was low enough to be light deficient for photosynthesis. After snow removal, there was a 67 % increase in the under-ice PAR (Fig. 2), resulting in deficiency for biomass accrual occurring 12 % of the 17 times measured, and only 6 % were deficient for photosynthesis if snow cover is absent.

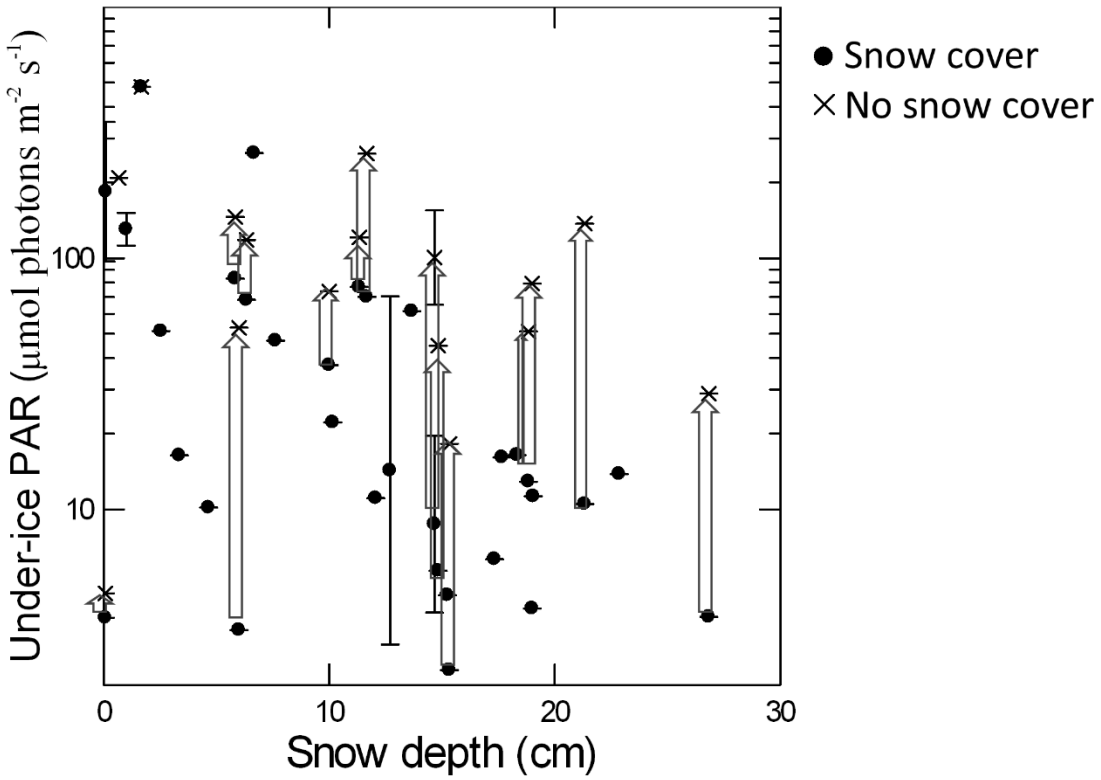

Figure 2. Impact of snow on under-ice photosynthetically active radiation (PAR). Shown are the mean and standard error of PAR readings (note log scale) at the ice-water interface as a function of snow depth for all water bodies and dates. Black circles represent under-ice PAR with ambient snow conditions, and "x"s show measurements taken after snow was physically removed. Arrows indicate increase in PAR after snow removal.

Surface or under-ice PAR is not entirely representative of the water column where phytoplankton are growing and photosynthesizing. $\bar{E}_{24}$ is used to represent the amount of light in the convective mixed layer over a 24-hour period and allows for comparison between open-water and under-ice seasons (Fig. 3; Tables 1 & 2). The highest $\bar{E}_{24}$ values (~ 92 μmol m^{-2} s^{-1}) occurred on Blackstrap and Broderick reservoirs during the open-water season and on Lake Simcoe under-ice. The lowest $\bar{E}_{24}$ values (~ 20 μmol m^{-2} s^{-1}) occurred on Blackstrap and Broderick reservoirs under-ice (Fig. 3; Table 1). Under-ice $\bar{E}_{24}$ was consistently (although not significantly) lower

than open-water, with the exception of Lake Simcoe, where we attribute the high under-ice $\bar{E}_{24}$ to the absence of snow cover resulting in shallow convective mixing depths (Pernica et al., 2017). Lake Simcoe under-ice $\bar{E}_{24}$ was significantly higher than the 3 Saskatchewan reservoirs (Table 2).

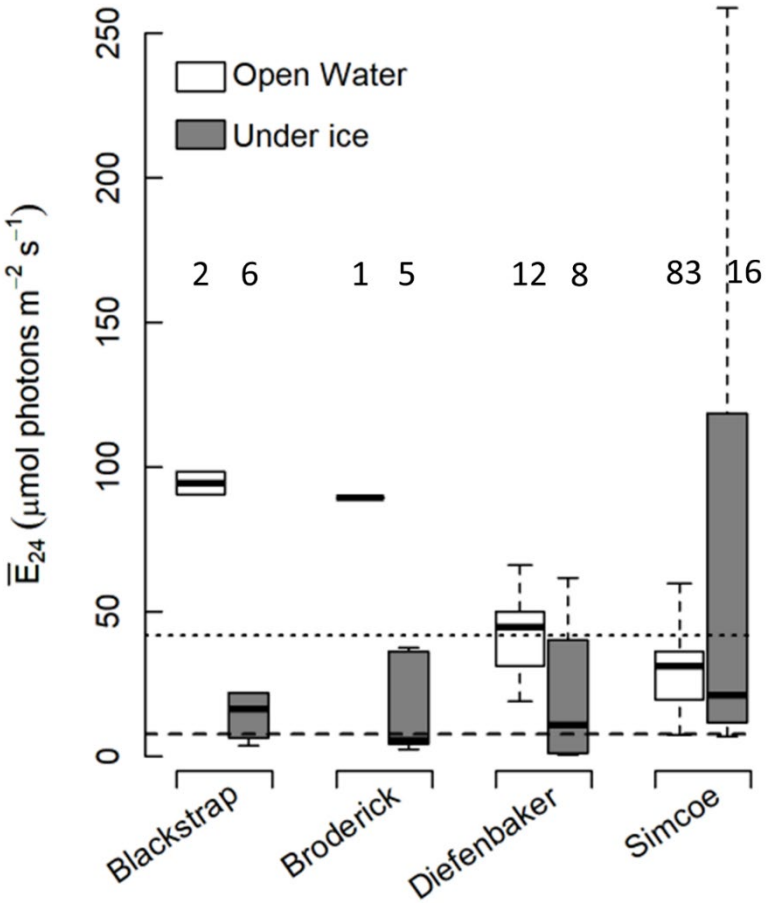

Figure 3. Comparison of the mean light experienced in the convective mixed layer by suspended phytoplankton over a 24-hour period ($\bar{E}_{24}$) between open-water (open boxes) and under-ice (grey boxes) for each of the 4 water bodies. Boxplots display the median of $\bar{E}_{24}$ with the first, and third quartiles, and whiskers indicate the minimum and maximum values. The numbers above the boxes indicate the *n* value. The top horizontal line at 41.7 µmol m^{-2} s^{-1} is the open-water light threshold (Hecky & Guildford, 1984) and the bottom horizontal line at 7.6 µmol m^{-2} s^{-1} is the under-ice light threshold (Gosselin et al., 1985).

Table 2. Two-way Analysis of Variance (ANOVA) and Tukey-Kramer *post hoc* comparisons between season (open-water and under-ice) and water body (Blackstrap, Broderick, Diefenbaker, Simcoe) for physical and biological parameters (Table 1). *Post-hoc* tests were conducted if ANOVA factors were identified as significant ($p < 0.05$). The letters for the *post-hoc* comparison indicate statistical significance ($p < 0.05$); the relationship between identical letters is not statistically significant, whereas the relationship between different letters is significant. $\bar{E}_{24}$, mean daily mixed layer irradiance; AGP, Areal Gross Productivity; ANP, Areal Net Productivity; AR, Areal Respiration; E_k, light saturation parameter; α, light-limited slope of the P-E curve.

Parameter				*Post-hoc* test		*Post-hoc* test			
				Open-water	Under-ice	Blackstrap	Broderick	Diefenbaker	Simcoe
$\bar{E}_{24}$	season		$F_{1,125}$=18.724, p<0.0005						
	water body		$F_{3,125}$=2.433, p=0.068						
	interaction		$F_{3,125}$=8.700, p<0.0005						
		open-water				a	a	a	a
		under-ice				ac	ab	a	c
		Blackstrap		a	a				
		Broderick		a	a				
		Diefenbaker		a	b				
		Simcoe		a	a				
AGP-$\delta^{18}O$	season		$F_{1,91}$=369.225, p<0.0005						
	water body		$F_{3,91}$=1.776, p=0.157						
	interaction		$F_{3,91}$=7.903, p<0.0005						
		open-water				a	ab	ab	b
		under-ice				a	a	a	a

		Blackstrap		a	b				
		Broderick		a	b				
		Diefenbaker		a	b				
		Simcoe		a	b				
ANP-$\delta^{18}O$	season		$F_{1,90}$=39.175, p<0.0005						
	water body		$F_{3,90}$=2.108, p=0.105						
	interaction		$F_{3,90}$=8.287, p<0.0005						
		open-water				a	ab	ab	b
		under-ice				a	b	a	a
		Blackstrap		a	b				
		Broderick		a	b				
		Diefenbaker		a	a				
		Simcoe		a	a				
AR-$\delta^{18}O$	season		$F_{1,91}$=200.805, p<0.0005						
	water body		$F_{3,91}$=17.172, p<0.0005						
	interaction		$F_{3,91}$=3.321, p=0.023						
		open-water				a	a	a	a
		under-ice				a	a	b	b
		Blackstrap		a	b				
		Broderick		a	a				
		Diefenbaker		a	b				
		Simcoe		a	b				
AGP:AR-$\delta^{18}O$	season		$F_{1,89}$=21.778, p<0.0005						
	water body		$F_{3,89}$=9.296, p<0.0005						
	interaction		$F_{3,89}$=16.180, p<0.0005						
		open-water				a	a	a	a
		under-ice				a	a	b	b
		Blackstrap		a	b				
		Broderick		a	b				
		Diefenbaker		a	a				
		Simcoe		a	a				
E_k	season		$F_{1,133}$=9.180, p=0.003						
	water body		$F_{3,133}$=28.102, p<0.0005						

	interaction		$F_{3,133}$=0.522, p=0.668						
		open-water				a	ab	a	b
		under-ice				a	a	a	b
		Blackstrap		a	a				
		Broderick		a	a				
		Diefenbaker		a	b				
		Simcoe		a	b				
α	season		$F_{1,133}$=0.576, p=0.449						
	water body		$F_{3,133}$=0.233, p=0.873						
	interaction		$F_{3,133}$=0.925, p=0.431						
$\bar{E}_{24}$:E_k	season		$F_{1,111}$=2.673, p=0.105						
	water body		$F_{3,111}$=10.235, p<0.0005						
	interaction		$F_{3,111}$=4.543, p=0.005						
		open-water				a	a	a	a
		under-ice				a	a	a	b
		Blackstrap		a	a				
		Broderick		a	a				
		Diefenbaker		a	a				
		Simcoe		a	a				

429

The maximum and minimum individual $\bar{E}_{24}$ values occur under-ice (Fig. 3, Table 1), with the maximum AGP_F occurring on Lake Diefenbaker during the open-water season, and the minimum under-ice on Broderick reservoir (Table 3). During the open-water season on all 4 water bodies, 74 % of the individual $\bar{E}_{24}$ values indicated light deficiency (<41.7 μmol m^{-2} s^{-1}, Hecky & Guildford, 1984); under-ice, 29 % indicated light deficiency (<7.6 μmol m^{-2} s^{-1}, Gosselin et al., 1985; Fig. 3).

Dissolved inorganic P and N concentrations can also limit productivity. Under-ice DRP, NH_4^+, and NO_3^- discrete sample (from 0–2 m) concentrations were 10x, 3x, and 59x higher than the open-water concentrations, respectively (Table 1). Under-ice DRP concentrations (mean= 0.18 μmol L^{-1}, Table 1) and dissolved inorganic nitrogen ($NH_4^+ + NO_3^-$) concentrations (mean= 9.7 μmol L^{-1}, Table 1) were sufficient relative to dissolved inorganic nutrient deficiency thresholds (Chorus & Spijkerman, 2021). The ratios of PN:PP were <22 in all water bodies and all seasons (Table 1), indicating P sufficiency.

3.2 Spatial and temporal variability in metabolism

Comparison of AGP, AR, ANP and the P:R ratio allows us to determine if water bodies are net autotrophic (P:R> 1) and dominated by primary productivity, or net heterotrophic (P:R< 1) and dominated by respiration. The $\delta^{18}O$-O_2 approach is the only method with both production and respiration rates in all 4 water bodies; this robust dataset was used to examine spatial (between water bodies and vertical [under-ice]) and temporal (open-water/under-ice and days since ice-on) metabolic rates. During the open-water season, the mean AGP-$\delta^{18}O$ rates for all 4 water bodies (35.8 mmol O_2 m^{-2} day^{-1}) is 81x higher than the mean under-ice rates (0.4 mmol O_2 m^{-2} day^{-1}; Table 3). Open-water mean AR-$\delta^{18}O$ rates for all 4 water bodies (32.1 mmol O_2 m^{-2} day^{-1}) is 8x higher than the mean under-ice rates (4.1 mmol O_2 m^{-2} day^{-1}; Table 3).

453 **Table 3. Method comparison between open-water and under-ice approaches to measuring**
454 **areal gross production (AGP) rates differentiated by water body. AGP rates are derived**
455 **from fluorometric (Fluoro) and $\delta^{18}O$ methods. Data were transformed and then analyzed**
456 **with a one-way ANOVA with method as factor. Bolded values are significantly different**
457 **($p<0.05$) and the higher rates are italicized. AGP arithmetic means are in units of mmol O_2**
458 **m^{-2} day^{-1}. NA, Not Applicable. *n = 1.**

	Blackstrap	**Broderick**	**Diefenbaker**	**Simcoe**
Open-water				
F-value	NA*	NA*	$F_{1,9}$=4.138	$F_{1,138}$=36.205
p-value			0.072	<0.0005
Method				
Fluoro	NA	43.0	264.3	***86.8***
$\delta^{18}O$	116.3	73.5	49.7	**31.9**
Under-ice				
F-value	$F_{1,13}$=4.200	$F_{1,9}$=40.190	$F_{1,15}$=43.606	$F_{1,30}$=13.760
p-value	0.061	<0.0005	<0.0005	0.001
Method				
Fluoro	44.2	***10.2***	***18.0***	***29.5***
$\delta^{18}O$	0.1	**0.2**	**0.5**	**0.9**

459

460 During the open-water season, all the water bodies were net autotrophic with AGP-$\delta^{18}O$
461 rates ranging from 116.3 (Blackstrap) to 31.9 mmol O_2 m^{-2} day^{-1} (Simcoe; Table 3; Fig. 4A).
462 ANP-$\delta^{18}O$ was significantly higher on Blackstrap (20.0 mmol O_2 m^{-2} day^{-1}) than Simcoe (2.9
463 mmol O_2 m^{-2} day^{-1}), while AR-$\delta^{18}O$ rates were not different between water bodies (Tables 1, 2 &
464 3; Fig. 4A). Under ice, Blackstrap and Broderick were heterotrophic, while Diefenbaker and
465 Simcoe were autotrophic (Table 1, Fig. 4B, Table 4). AGP-$\delta^{18}O$ rates were low (0.4 mmol O_2 m^{-2}
466 day^{-1} mean for all water bodies) and not significantly different between water bodies (Tables 2 &
467 3; Fig. 4B). Under-ice ANP-$\delta^{18}O$ rates were significantly lower on Broderick (-12.9 mmol O_2 m^{-2}
468 day^{-1}) than the other water bodies (mean of -1.7 mmol O_2 m^{-2} day^{-1}). AR-$\delta^{18}O$ was significantly
469 higher on Blackstrap and Broderick (mean of 8.2 mmol O_2 m^{-2} day^{-1}) than Diefenbaker and
470 Simcoe (mean of 0.6 mmol O_2 m^{-2} day^{-1}; Tables 2 & 3; Fig. 4B). Open-water AGP-$\delta^{18}O$ was
471 significantly higher than under-ice for all 4 water bodies (Table 4). Open-water ANP-$\delta^{18}O$ was
472 significantly higher on Blackstrap and Broderick than under-ice rates; seasonal rates were similar
473 on Diefenbaker and Simcoe. Open-water AR-$\delta^{18}O$ was significantly higher than under-ice for all
474 water bodies with the exception of Broderick (Tables 2, 3 & 4; Fig. 4).

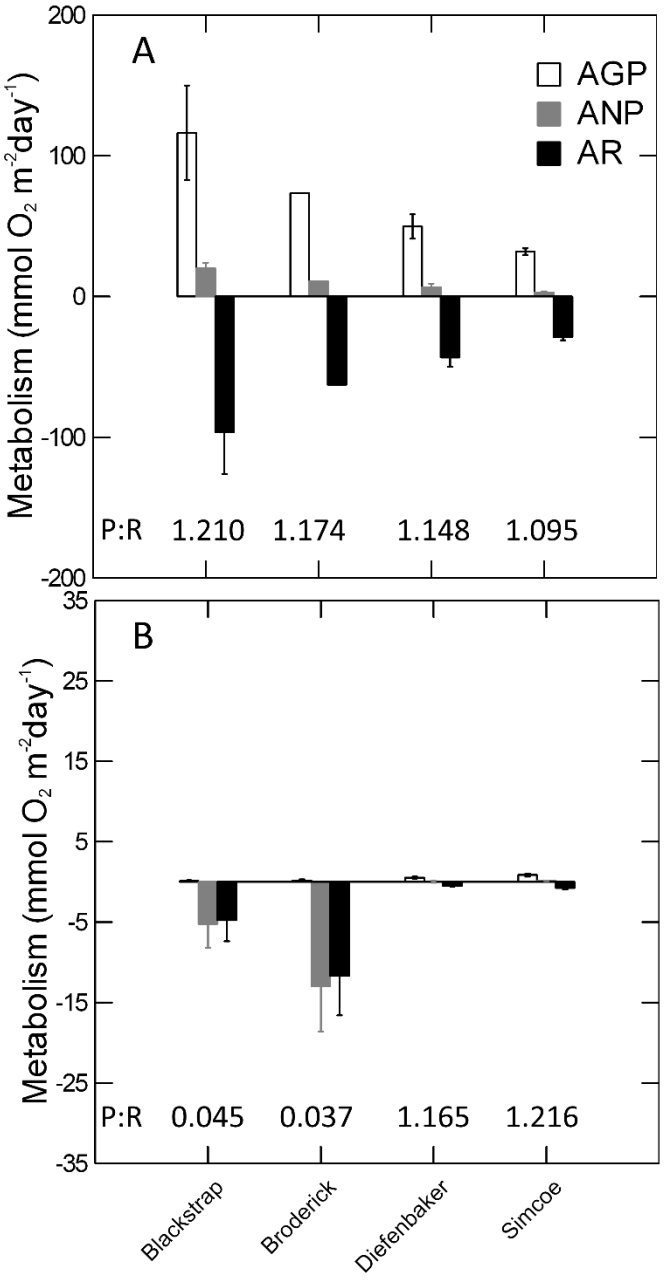

475

476 **Figure 4. Comparison of metabolic rates between the 4 study water bodies. A) Open-water**
477 **areal gross production (AGP- $\delta^{18}O$), areal net production (ANP- $\delta^{18}O$), and areal**
478 **respiration (AR- $\delta^{18}O$) rates. B) Under-ice AGP- $\delta^{18}O$, ANP- $\delta^{18}O$, and AR- $\delta^{18}O$ rates. The**
479 **AGP:AR- $\delta^{18}O$ (P:R) ratios for each water body and both seasons are shown as text. Bars**
480 **display the mean and standard error of the metabolic rates. Note the different y-axis scales.**

Table 4. Literature review of open-water (OW) and under-ice (UI) areal gross production (AGP) and areal respiration (AR) ratios. For different approaches to measuring AGP and AR on the same water samples, ranges (minimum-maximum) are reported, otherwise, shown are the means. Ratios were collected directly from text or estimated via table values or by digitizing figures. Given the diversity of methods and units and thus, the inherent assumptions that must be made to convert between methods, we chose to report rates as ratios and avoided comparing our absolute rates with published rates.

Water body	Location	Latitude °N	OW:UI AGP	OW:UI AR	OW AGP:AR	UI AGP:AR	Year-round AGP:AR	Citation
Char	Canada	74.7053	2					Kalff & Welch, 1974
Meretta	Canada	74.7009	~1					Kalff & Welch, 1974
Võrtsjärv	Estonia	58.3104	4					Noges & Noges, 1999
Winnipeg	Canada	53.2977			0.8		0.9	Wassenaar, 2012
Blackstrap	Canada	51.7848	8	20	1.2	0.0	0.3	This study
Broderick	Canada	51.4727	12	5	1.2	0.0	1.2	This study
Diefenbaker	Canada	51.1785	13–186	85	1.1	1.2	1.2	This study
Simoncouche	Canada	48.2307	73					Grosbois et al., 2020
Neusiedler	Hungary	47.8650	6					Dokulil et al., 2014
Balaton	Hungary	46.8303	6					Dokulil et al., 2014
Georgetown	US	46.1812			1.0	0.6	0.8	Gammons et al., 2014
Wintergreen	US	45.9018	2					Wetzel, 2001
Calvert	US	45.8391			1.1	0.6	0.8	Gammons et al., 2013
Simcoe	Canada	44.4636	1–6	33	1.1	1.2	1.1	This study
Simcoe	Canada	44.4636	5					Kim et al., 2015
Santo	Italy	44.4026	6					Camurri et al., 1976; Ferrari, 1976
Ontario	Canada/US	43.6333	2.5					Glooschenko et al., 1974
Michigan	Canada/US	43.4501	~1					Biddanda & Cotner, 2002
Sunapee	US	43.3802		0.8				Brentrup et al., 2021
Erie	Canada/US	42.0669	3					Depew et al., 2006
Erie	Canada/US	42.0669	2					Saxton et al., 2012

Erie	Canada/US	42.0669	~1					D'souza, 2012
Sylvan	US	41.4872	6					Wetzel, 1966
Lawrence	US	41.2956	6					Wetzel, 2001
Goose	US	41.2382	5					Wetzel, 1966
Falling Creek	US	37.3000	2	3	0.8	1.0	0.8	Howard et al., 2024
Haruna	Japan	36.4764	~1					Maeda & Ichimura, 1973
Druzhby	Antarctica	-68.5931	0.3					Henshaw & Laybourn-Parry, 2002

Under-ice AGP:AR-$\delta^{18}O$ decreased with depth in Lakes Diefenbaker and Blackstrap (Fig. 5). While the P:R ratio is less than one throughout the water column on Blackstrap, Broderick, and Diefenbaker, Lake Simcoe is net autotrophic during the winter at all sampling depths (Figs 5 & 6), likely driven by high $\bar{E}_{24}$ values (Fig. 3). Just under the ice surface, Lake Diefenbaker is also net autotrophic, but P:R was usually less than one below 7.5 m depth (Fig. 5). In Blackstrap and Broderick, it is the AR-$\delta^{18}O$ that is increasing with depth. From the surface to 6 m, AR-$\delta^{18}O$ increased from 0.5 to 25.9 mmol O_2 m^{-2} day^{-1} in Blackstrap, and from zero to 59.7 mmol O_2 m^{-2} day^{-1} in Broderick. In Diefenbaker, the decrease in AGP:AR-$\delta^{18}O$ with depth is primarily driven by decreases in AGP-$\delta^{18}O$, which is as high as 1.1 mmol O_2 m^{-2} day^{-1} at the surface, and zero below 20 m. AR-$\delta^{18}O$ is consistently zero throughout the water column in both Diefenbaker and Simcoe. In Simcoe, AGP-$\delta^{18}O$ rates are also consistent with depth, only ranging from 0.4–0.7 mmol O_2 m^{-2} day^{-1} throughout the water column. In Simcoe, the average under-ice $\bar{E}_{24}$ value of 40.6 (range: 6.9–555.6 µmol m^{-2} s^{-1}) is significantly higher than Diefenbaker (mean: 42.5, range: 0.5–223.0 µmol m^{-2} s^{-1}) and Broderick (mean: 29.2, range: 2.3–89.5 µmol m^{-2} s^{-1}; Tables 1 & 2, Fig. 3) and well above the light deficiency threshold (7.6 µmol m^{-2} s^{-1}, Gosselin et al., 1985; Fig. 3). The deep euphotic zone under-ice in Lake Simcoe appears to facilitate photosynthesis down to depths as deep as 35 m.

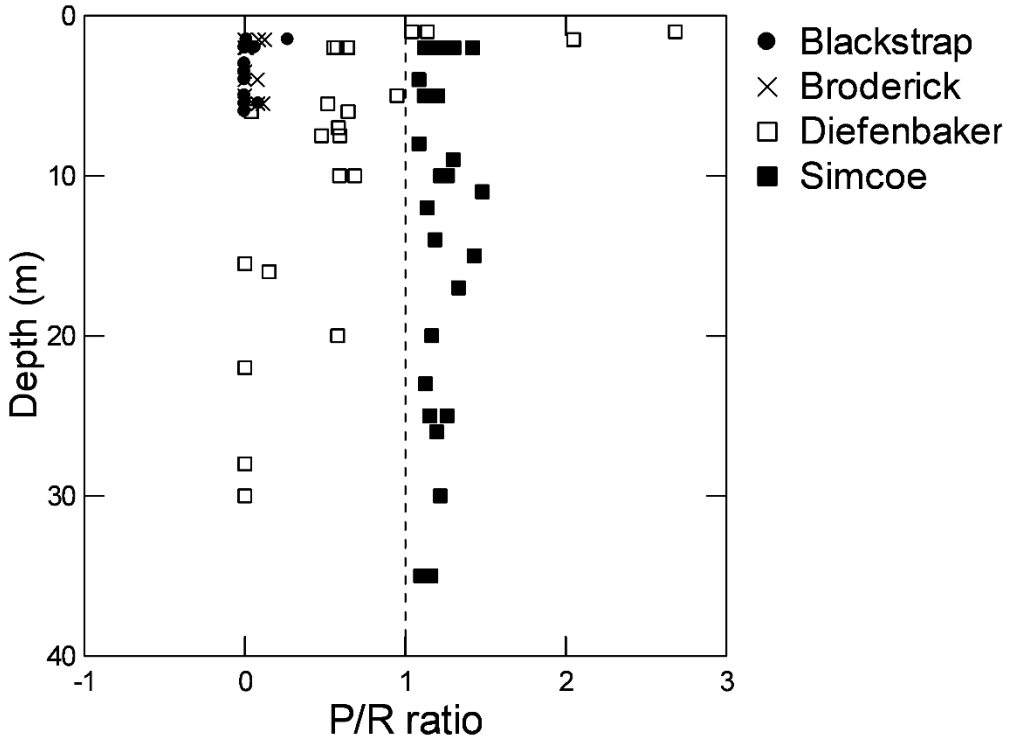

Figure 5. The vertical distribution of the under-ice AGP:AR- $\delta^{18}O$ (P:R) ratios differentiated by water body. Symbols left of the vertical line at one indicate heterotrophy, while symbols on the right of the line indicate autotrophy.

All of the water bodies were sampled multiple times over the winter, allowing us to examine relationships between days since ice-on and metabolism (Fig. 6). There were no relationships between AGP-$\delta^{18}O$ nor AR-$\delta^{18}O$ and days since ice-on for any of the water bodies; however, on Lake Simcoe, there was a negative relationship between days since ice on and snow depth (r= -0.917, p= 0.007, n= 9). Wind-swept conditions on a large lake such as Simcoe result in negligible snow cover at the end of the winter (Table 1). On the last day of safe sampling on the ice at station K42 of Lake Simcoe (Fig. 1) on March 14th 2011, we recorded the maximum under-ice Chl *a* concentration (13.1 µg L^{-1}; Table 1) that extended 15 m deep in the water column (Pernica et al., 2017). Surface water phytoplankton biomass was 1,577.00 mg m^{-3} and

517 was composed primarily of a small centric diatom (*Stephanodiscus*). This Chl *a* peak
518 corresponded with the maximum under-ice fluorometric AGP rates for Lake Simcoe (AGP_F:
519 271.7 mmol O_2 m^{-2} day^{-1}; Table 3). The AGP-$\delta^{18}O$ rates on this date and station (1.2 mmol O_2 m^{-2} day^{-1}) were slightly lower than the maximum of 1.9 mmol O_2 m^{-2} day^{-1} (Table 3).

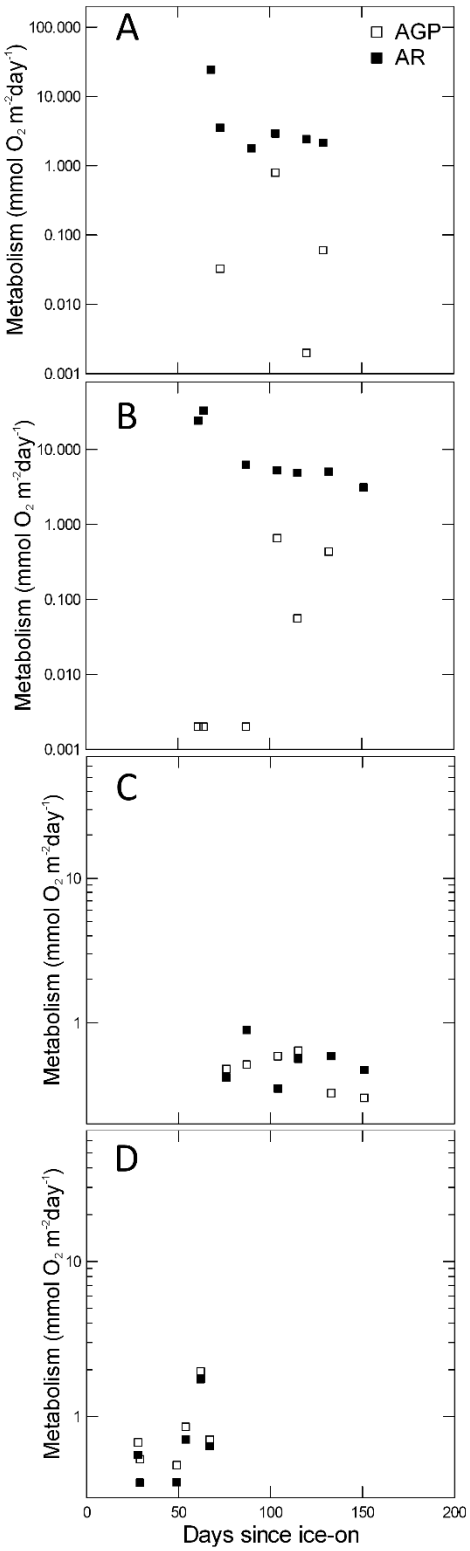
A
B
C
D
AGP
AR
Metabolism (mmol O2 m-2day-1)
100.000
10.000
1.000
0.100
0.010
0.001
10
1
0
50
100
150
200
Days since ice-on

521

Figure 6. Under-ice metabolic rates over the winter season (days since ice-on). Shown are individual rates of areal gross production (AGP- $\delta^{18}O$) and areal respiration (AR- $\delta^{18}O$) from 2 m water samples. A) Blackstrap, B) Broderick, C) Diefenbaker, D) Simcoe.

3.3 Comparison of production methods

We applied 2 different methods for measuring AGP rates (Table 3). The ratio between the different open-water AGP methods was 4.3 (Fluoro: $\delta^{18}O$, 0.1–24.8, *n*= 60; Table 3). The methodological differences between AGP_F and AGP-$\delta^{18}O$ were insignificant for Lake Diefenbaker. On Lake Simcoe, the AGP_F method yielded significantly higher rates than the AGP-$\delta^{18}O$ method (Table 3).

Estimates of under-ice AGP ratios were 399.0 (Fluoro: $\delta^{18}O$, 0.4–4,507.2, *n*= 25; Table 3). With the exception of Blackstrap, the rest of the water bodies had significant differences between AGP_F and AGP-$\delta^{18}O$, with AGP_F being consistently higher on every water body. On Blackstrap and Diefenbaker, we also estimated under-ice respiration rates using continuous O_2 sensors and the free-water approach (Solomon et al., 2013). AR ratios ($\delta^{18}O$:free-water) were 0.5 and 0.007, respectively (Supplemental Information).

3.4 Physiological light response variables

The P-E parameter, E_k, is the light saturation parameter and can serve as an indicator of the phytoplankton community's capacity for light. The open-water E_k values on Lake Simcoe were significantly lower than both Blackstrap and Diefenbaker, and under ice they were significantly lower than all of the SK reservoirs (Tables 1 & 2). Open-water and under-ice E_k values were similar on Blackstrap and Broderick but were significantly higher during the open-water season than under-ice on Lakes Diefenbaker and Simcoe (Tables 1 & 2). The E_k values can be compared to the light intensity thresholds for the open-water season (<41.7 μmol m^{-2} s^{-1}; Hecky &

Guildford, 1984) and under-ice (<7.6 μmol m^{-2} s^{-1}; Gosselin et al., 1985). During the open-water season, E_k values on Broderick, Diefenbaker, and Simcoe were 8, 10, and 3 x higher, respectively, than the 41.7 μmol m^{-2} s^{-1} threshold (Hecky & Guildford, 1984). Under ice, E_k values on Blackstrap, Broderick, Diefenbaker, and Simcoe were 30, 41, 30, and 10 x higher, respectively, than the 7.6 μmol m^{-2} s^{-1} threshold (Gosselin et al., 1985). Across all water bodies, under-ice E_k is 21x higher than the threshold, and open-water E_k is 4x times higher than the threshold, suggesting that if light conditions improve, winter phytoplankton will respond ~5x more strongly than summer phytoplankton communities. The light-limited slope of the P-E curve (α) was similar across water bodies and between seasons (Tables 1 & 2).

The ratio of $\bar{E}_{24}/E_k$ can also serve as an indicator of light deficiency with a threshold of one (Hecky & Guildford, 1984). This ratio is <1 consistently for all water bodies and both seasons with the exception of Lake Simcoe under-ice, which has a significantly higher ratio than the SK reservoirs (Tables 1 & 2). The $\bar{E}_{24}/E_k$ ratios were similar between seasons.

3.5 Photoacclimation

Phytoplankton acclimate to lower light by increasing their light harvesting pigments such as Chl *a* (Arrigo et al., 2010). Given the significant differences in light between water bodies and seasons (Tables 1 & 2, Fig. 3), we are cognizant that Chl *a* may not consistently serve as a proxy for phytoplankton biomass. We measured both phytoplankton biomass and particulate organic C (POC) and assessed their relationships to Chl *a*; photoacclimation could be occurring if there is a weak relationship between Chl *a* and biomass or POC. There was never a relationship between Chl *a*, biomass, nor POC for Blackstrap and Broderick under-ice (Table 5). In Lake Diefenbaker, Chl *a* and POC were significantly, positively related during the open-water season, but not under ice. There was, however, a significant positive relationship between Chl *a* and biomass, and POC and biomass, indicating photoacclimation may not be occurring under-ice on Lake Diefenbaker.

In Lake Simcoe, while the relationship between Chl *a* and POC was strong during the open-water season, it weakened during the winter (Table 5). The poor under-ice relationships between Chl *a*, phytoplankton biomass, and POC indicates that photoacclimation is occurring under the low light conditions of the under-ice season; therefore, Chl *a* is an unsuitable proxy for phytoplankton biomass in the winter.

574 **Table 5. Linear regressions between Chlorophyll *a* (Chl *a*), Particulate Organic Carbon (POC), and phytoplankton biomass**
575 **(Phyto) differentiated by water body and open-water and ice-covered seasons. Relationships where *n*< 3 were excluded.**
576 **Significant relationships are identified with bolded R^2_{adj} values.**

Water body	**Season**		Chl *a*	POC
Blackstrap	Under-ice	POC	R^2_{adj}= 0.000, *p*= 0.968, *n*= 7	
		Phyto	R^2_{adj}= 0.000, *p*= 0.386, *n*= 8	R^2_{adj}= 0.000, *p*= 0.726, *n*= 7
Broderick	Under-ice	POC	R^2_{adj}= 0.243, *p*= 0.296, *n*= 4	
		Phyto	R^2_{adj}= 0.000, *p*= 0.775, *n*= 4	R^2_{adj}= 0.000, *p*= 0.655, *n*= 4
Diefenbaker	Open-water	POC	R^2_{adj}= **0.630**, *p*= 0.001, *n*= 12	
	Under-ice	POC	R^2_{adj}= 0.087, *p*= 0.245, *n*= 8	
		Phyto	R^2_{adj}= **0.518**, *p*= 0.027, *n*= 8	R^2_{adj}= **0.434**, *p*= 0.045, *n*= 8
Simcoe	Open-water	POC	R^2_{adj}= **0.174**, *p*< 0.0005, *n*= 88	
	Under-ice	POC	R^2_{adj}= 0.140, *p*= 0.058, *n*= 20	

577

4 Discussion

Year-round P:R ratios are close to unity, with autotrophy dominating in the open-water season and heterotrophy under ice. The depth of snow cover dictates the under-ice PAR (Pernica et al., 2017). On Lake Simcoe, snow depth decreased over the winter, resulting in the highest AGP rates on the last date of winter sampling (North et al., 2023). This coincided with the maximum Chl *a* concentration. When the snow is removed, there is a 67 % increase in under-ice PAR; the winter phytoplankton communities appear to be physiologically poised to respond to increases in light, with potential increases in productivity. While open-water and under-ice $\bar{E}_{24}$ values were not significantly different, a third of the time under-ice PAR was below the light deficiency threshold for phytoplankton. Changes in under-ice light, therefore, will have a profound influence on under-ice metabolism, with consequent effects on year-round lake function. Given the overriding effect of snow on PAR, snow appears to be a keystone winter variable, influencing in-lake metabolism.

4.1 How do under-ice rates of productivity and respiration compare with open-water rates?

Open-water AGP in our water bodies for both methods ranged from 1–186x higher than the under-ice rates (Table 4). Comparison of summer and winter production rates on the Laurentian Great Lakes (summarized in Ozersky et al., 2021) ranged from no differences on Lakes Michigan (Biddanda & Cotner, 2002) and Erie (D'souza, 2012) to 3x higher in the eastern basin of Lake Erie (Depew et al., 2006). The open-water to under-ice AGP ratio varies from less than one (0.3) in an Antarctic lake (Henshaw & Laybourn-Parry, 2002) to 73 in a Canadian lake (Grosbois et al., 2020) with the average ratio (excluding this study) of 7 (Table 4). Open-water AR for our 4 water bodies ranged from 5–85x higher than the under-ice rates (Table 4). The

601 opposite was found in an oligotrophic lake, where under-ice respiration was 1.2 times higher
602 than summer respiration (Brentrup et al., 2021). During the open-water season, the AGP:AR
603 ratio was on average higher than unity in our study systems, averaged around one for 2 US lakes
604 (Gammons et al., 2013, 2014), and was less than one on Canadian Great Lake Winnipeg
605 (Wassenaar, 2012). Under ice, our AGP:AR ratio was 0.67, with an average ratio of 0.6 for 2 US
606 lakes (Gammons et al., 2013, 2014), indicating heterotrophy was dominant in the winter. Net
607 heterotrophy was also reported for Lake Tovel (Italy) with the use of high frequency under-ice
608 O_2 sensors (Obertegger et al., 2017).

609 The year-round AGP:AR ratio ranges from 0.3 to 1.2 for our study systems, while the
610 only 4 other lakes with comparable ratios average less than one (0.8; Table 4). Given that our
611 ratios averaged around one (0.97), this likely is a delicate balance that can shift from year-to-
612 year, depending on the length and severity of winter conditions and subsequent light
613 environment. In Canadian water bodies, including a Saskatchewan reservoir (Finlay et al., 2019),
614 year-round CO_2 budgets revealed positive net annual CO_2 fluxes, indicating heterotrophy. The
615 under-ice CO_2 accumulation accounted for 3–80 % (Ducharme-Riel et al., 2015) and 31–64 %
616 (Finlay et al., 2019) of the annual CO_2 flux. Long-term analysis suggests that antecedent
617 seasonal conditions explained the 64 % efflux that occurred in the spring after ice-off (Finlay et
618 al., 2019). The paucity of published year-round rates makes it difficult to conclude whether most
619 lakes are net autotrophic or heterotrophic. When measured, winter metabolism is an important
620 component of annual O_2 and CO_2 lake budgets, but winter gas releases to the atmosphere tend to
621 be stochastic and brief (Ducharme-Riel et al., 2015) and would not be captured in typical
622 monthly monitoring programs.

623 4.2 Methodological caveats

Comparison of the 2 different methods used to measure AGP revealed some significant differences, which captures the spatial and temporal integration features and assumptions made with different approaches (Table 3). Incorporating multiple approaches and assumptions is the strength of our message. We also made comparisons regardless of the aquatic organisms present, differences in physical factors (i.e., wind) and water column mixing, and inherent assumptions of each technique including conversion factors. The Water-PAM fluorometer measures PSII quantum efficiency and is useful in estimating gross primary production but not respiration. The $\delta^{18}O$ approach accounts for all changes in O_2, which could be attributed to heterotrophic bacterioplankton, zooplankton <200 μm, as well as phytoplankton (which includes prokaryotic cyanobacteria) and processes such as nitrification, known to be important under-ice (Powers et al., 2017). The conversion factors between the various definitions of GPP (e.g., electron transport as measured by variable fluorescence versus gross O_2 evolution) and the variety of assumptions inherent to each technique (e.g., artifacts of non-phytoplankton respiration) also contribute to the methodological differences.

4.3 What are the environmental drivers of under-ice production and respiration rates?

As found here, nutrient deficiency is uncommon during the winter and shoulder seasons (Davies et al., 2004; Twiss et al., 2012) and light is most often the limiting factor to phytoplankton (Dokulil et al., 2014; Hampton et al., 2017; Pernica et al., 2017). During the open-water season, both Lakes Simcoe and Diefenbaker are P deficient (Dubourg et al., 2015; Guildford et al., 2013), and dissolved nutrient concentrations are much lower than under-ice (Table 1). We do not expect, therefore, that the under-ice phytoplankton community is nutrient limited (but see Knoll et al., 2023).

Under-ice, primary production typically occurs at the surface of the water column (Yoshida et al., 2003); both phytoplankton biomass (Lenard, 2015) and production (Dokulil et al., 2014) can be limited by light and respond quickly to improved light conditions (Hrycik & Stockwell, 2020). The under-ice light environment (estimated by $\bar{E}_{24}$) is dictated by convective mixing dynamics (Yang et al., 2020), where convective cells maintain the phytoplankton at the top of the water column (Bertilsson et al., 2013), improving the $\bar{E}_{24}$ (Bouffard et al., 2019; Pernica et al., 2017), resulting in increased phytoplankton biomass (Suarez et al., 2019). This is now a well-documented phenomenon on Lake Simcoe (Pernica et al., 2017), related to winter phytoplankton peaks (Baranowska et al., 2013; Yang et al., 2017). Our companion studies on Lake Simcoe documented these under-ice phytoplankton blooms that were 10 m thick (Pernica et al., 2017) and composed of small centric diatoms (e.g., *Stephanodiscus*), representing 3x more biomass in a single event than measured during the summer sampling (Kim et al., 2015). Late winter phytoplankton peaks related to improved light conditions have also been reported in Placid Lake, Montana, US (Baehr & DeGrandpre, 2004). The difference between open-water and under-ice $\bar{E}_{24}$ were only significant on Lakes Diefenbaker and Simcoe in our dataset. In 6 European shallow lakes, winter Secchi depths were similar, if not greater, than summer depths (Dokulil et al., 2014). Only 29 % of our under-ice samples indicated light deficiency, and Lake Simcoe demonstrated improved light conditions just prior to ice-off, which resulted in a Chl *a* peak and maximum AGP rates. Similar late winter/early spring under-ice phytoplankton peaks have also been observed on another Saskatchewan reservoir (Cavaliere & Baulch, 2020) and Lake Baikal, Russia (Katz et al., 2015). In Lake Sunapee, US, increases in productivity are implied by the O_2 increase at the end of winter and subsequent shift to autotrophy (Brentrup et

668 al., 2021). Ice duration was found to be an important factor in this shift, where ice-on and ice-off
669 periods were drivers of annual metabolism estimates (Brentrup et al., 2021).

670 Phytoplankton response to light can be assessed with P-E parameters that quantitatively
671 describe aspects of phytoplankton photophysiology. Fluorescence-based measurements have
672 previously been used to assess photosynthetic potential of winter phytoplankton in Lake Erie
673 (Edgar et al., 2016; Twiss et al., 2012) and in ice-covered reservoirs in the Czech Republic
674 (McKay et al., 2015). Consistent with our results, these studies found that winter phytoplankton
675 are photosynthetically active and physiologically robust (Edgar et al., 2016; McKay et al., 2015;
676 Twiss et al., 2012). The light saturation parameter, E_k, is an indicator of the phytoplankton
677 community's photoacclimation status. If the ratio of $\bar{E}_{24}/E_k$ is less than one, light deficient
678 conditions are expected. This was the case for 3 of our water bodies under ice cover, with the
679 fourth (Lake Simcoe) showing an $\bar{E}_{24}/E_k$ ratio of 1.4 (Table 1). During the winter, phytoplankton
680 acclimate to low-light conditions, as evidenced by low E_k values on Lake Balaton (55.9 µmol m^{-2}
681 s^{-1}) and Neusiedler See (30 µmol m^{-2} s^{-1}; Dokulil et al., 2014); considerably lower than our
682 winter E_k values which ranged from 78.7–354.2 µmol m^{-2} s^{-1} (Table 1). In ice-covered Lake Erie,
683 E_k was lower still (~10 µmol m^{-2} s^{-1}, Edgar et al., 2016). Winter-to-summer comparisons on Lake
684 Balaton and Neusiedler See demonstrated that E_k was 6x lower in the winter (Dokulil et al.,
685 2014), while in our dataset, E_k was only 2x lower in the winter. In these European lakes, P_{max} was
686 6x lower in winter than summer (Dokulil et al., 2014), while in our data set, $rETR_{max}$ was only 4x
687 lower in winter (Table 1). Under-ice phytoplankton populations in our study ecosystems have
688 adjusted to the low light environment by photoacclimating, which is reflected by the lack of
689 relationship between POC and Chl *a* concentrations. Our demonstration that Chl *a* does not
690 represent phytoplankton biomass in the winter is supported by other studies that showed

691 discrepancies between phytoplankton biomass and Chl *a* concentrations in under-ice samples
692 (Lenard, 2015). Photoacclimation has implications for broader applications such as winter
693 limnology studies where Chl *a* is assumed to represent under-ice algal biomass (Hampton et al.,
694 2017).

695 4.4 What can we expect in a warmer and ice-free future?

696 Overlaid on the climate-induced reductions in ice cover (Sharma et al. 2019), climate predictions
697 also suggest that there will be less snow cover (both depth and duration; DeBeer et al., 2016). Ice
698 and snow removal experiments provide some insights into what this means for future lake
699 metabolism and the role that temperate lakes play in global carbon budgets. In an experimental
700 study when 50 % of the ice cover was removed, a significant decrease in GPP occurred (Hamdan
701 et al., 2018), likely related to changes in convective mixing and the resultant light environment.
702 The importance of snow on under-ice metabolism has been established (Obertegger et al., 2017);
703 experimental snow removal resulted in an increase in AGP (Garcia et al., 2019). Increased
704 production will result in increased O_2 concentrations, which may prevent winter fish kills. An
705 increase in phytoplankton lipids will also support winter zooplankton populations (Grosbois et
706 al., 2017; Hrycik et al., 2017), which will support fish and increase aquatic biodiversity (Hrycik
707 et al., 2017; McMeans et al., 2017). Temporal changes in phytoplankton peaks as a result of
708 changing winters could also cause potential shifts in lake ecology. For example, a temporal
709 mismatch between phytoplankton peaks and zooplankton egg hatching could result in cascading
710 effects in food webs.

711 Here, we advance our understanding of winter limnology under a changing climate.
712 Transient peaks in biomass and production matter, and should be considered in predictive lake

713 models. The current lack of year-round data is a major impediment to predict the effect of a
714 changing climate on lake ecology and biogeochemistry.

715 **Open Research**

716 The data used in the study are available at the Environmental Data Initiative (EDI) via
717 https://doi.org/10.6073/pasta/ac92e6eb81acf4b3d6701aa296550dc2 (Accessed 2023-01-30). This
718 is cited in the manuscript as North et al., 2023.

719 *North, R.L., J.J. Venkiteswaran, G. Silsbe, J.W. Harrison, J.J. Hudson, R.E. Smith, P.J. Dillon,
720 P.J. Pernica, S.J. Guildford, M. Kehoe, and H.M. Baulch. 2023. Year-round metabolism data
721 from Lakes Simcoe (Ontario, 2010-2011), Diefenbaker, Blackstrap, and Broderick
722 (Saskatchewan, 2013-2014), Canada. ver 2. Environmental Data Initiative.
723 https://doi.org/10.6073/pasta/ac92e6eb81acf4b3d6701aa296550dc2 (Accessed 2023-01-30).

724

References

Adrian, R, Deneke, R., Mischke, U., Stellmacher, R., & Lederer, P. (1995). A long-term study of the Heliligensee (1975-1992). Evidence for effects of climate change on the dynamics of eutrophied lake ecosystems. *Archiv Fur Hydrobiologie*, *133*(3), 315–337.

Adrian, Rita, Walz, N., Hintze, T., Hoeg, S., & Rusche, R. (1999). Effects of ice duration on plankton succession during spring in a shallow polymictic lake. *Freshwater Biology*, *41*(3), 621–632. https://doi.org/10.1046/j.1365-2427.1999.00411.x

Arrigo, K. R., Mills, M. M., Kropuenske, L. R., Van Dijken, G. L., Alderkamp, A. C., & Robinson, D. H. (2010). Photophysiology in two major southern ocean phytoplankton taxa: Photosynthesis and growth of phaeocystis antarctica and fragilariopsis cylindrus under different irradiance levels. *Integrative and Comparative Biology*, *50*(6), 950–966. https://doi.org/10.1093/icb/icq021

Bachmann, R. W., & Canfield, D. E. (1996). Use of an alternative method for monitoring total nitrogen concentrations in Florida lakes. *Hydrobiologia*, *323*(1), 1–8.

Baehr, M. M., & DeGrandpre, M. D. (2004). In situ pCO(2) and O-2 measurements in a lake during turnover and stratification: Observations and modeling. *Limnology and Oceanography*, *49*(2), 330–340.

Baranowska, K. A., North, R. L., Winter, J. G., & Dillon, P. J. (2013). Long-term seasonal effects of dreissenid mussels on phytoplankton in Lake Simcoe, Ontario, Canada. *Inland Waters*, *3*(2), 285–296. https://doi.org/10.5268/IW-3.2.527

Belzile, C., Vincent, W. F., Gibson, J. A. E., & Van Hove, P. (2001). Bio-optical characteristics of the snow, ice, and water column of a perennially ice-covered lake in the High Arctic. *Canadian Journal of Fisheries and Aquatic Sciences*, *58*(12), 2405–2418. https://doi.org/10.1139/cjfas-58-12-2405

747 Benson, B., & Krause, D. J. (1984). The concentration and isotopic fractionation of oxygen dissolved in
748 freshwater and seawater in equilibrium with the atmosphere. *Limnol. Oceanogr.*, *29*(3), 620–
749 632.
750 Benson, B., Krause, D. J., & Peterson, M. (1979). The solubility and isotopic fractionation of gases in
751 dilute aquatic solution I. Oxygen. *J Solution Chem*, *8*, 655–690.
752 Bergmann, M., & Peters, R. H. (1980). A simple reflectance method for the measurement of particulate
753 pigment in lake water and its application to phosphorus-chlorophyll-seston relationship.
754 *Canadian Journal of Fisheries and Aquatic Sciences*, *3*, 111–114. https://doi.org/10.1139/f80-011
755 Bertilsson, S., Burgin, A., Carey, C. C., Fey, S. B., Grossart, H.-P., Grubisic, L. M., et al. (2013). The under-
756 ice microbiome of seasonally frozen lakes. *Limnology and Oceanography*, *58*(6), 1998–2012.
757 https://doi.org/10.4319/lo.2013.58.6.1998
758 Biddanda, B. A., & Cotner, J. B. (2002). Love handles in aquatic ecosystems: The role of dissolved organic
759 carbon drawdown, resuspended sediments, and terrigenous inputs in the carbon balance of
760 Lake Michigan. *Ecosystems*, *5*, 431–445.
761 Block, B. D., Denfeld, B. A., Stockwell, J. D., Flaim, G., Grossart, H. P. F., Knoll, L. B., et al. (2019). The
762 unique methodological challenges of winter limnology. *Limnology and Oceanography: Methods*,
763 *17*(1), 42–57. https://doi.org/10.1002/lom3.10295
764 Bocaniov, S A, & Smith, R. E. H. (2009). Plankton metabolic balance at the margins of very large lakes:
765 temporal variability and evidence for dominance of autochthonous processes. *Freshwater*
766 *Biology*, *54*, 345–362. https://doi.org/doi: 10.1111/j.1365-2427.2008.02120.x
767 Bocaniov, Serghei A., Schiff, S. L., & Smith, R. E. H. (2015). Non steady-state dynamics of stable oxygen
768 isotopes for estimates of metabolic balance in large lakes. *Journal of Great Lakes Research*,
769 *41*(3), 719–729. https://doi.org/10.1016/j.jglr.2015.05.013

Bouffard, D., Zdorovennova, G., Bogdanov, S., Efremova, T., Lavanchy, S., Palshin, N., et al. (2019). Under-ice convection dynamics in a boreal lake. *Inland Waters*, *9*(2), 142–161. https://doi.org/10.1080/20442041.2018.1533356

Brentrup, J. A., Richardson, D. C., Carey, C. C., Nicole, K., Bruesewitz, D. A., Weathers, K. C., et al. (2021). Under-ice respiration rates shift the annual carbon cycle in the mixed layer of an oligotrophic lake from autotrophy to heterotrophy. *Inland Waters*, *11*(1), 114–123. https://doi.org/10.1080/20442041.2020.1805261

Butts, E., & Carrick, H. J. (2017). Phytoplankton seasonality along a trophic gradient of temperate lakes: Convergence in taxonomic compostion during winter ice-cover. *Northeastern Naturalist*, *24*, B167–B187. https://doi.org/10.1656/045.024.s719

Camurri, I., Ferrari, I., & Villani, M. (1976). Biomassa e produczione del fitoplancton nel lago Santo Parmense nella stagione delle acque aperte. *Arch. Oceanogr. Limnol.*, *18*, 237–253.

Cavaliere, E, & Baulch, H. M. (2018). Denitrification under lake ice. *Biogeochemistry*, *137*(3), 285–295. https://doi.org/10.1007/s10533-018-0419-0

Cavaliere, Emily, & Baulch, H. M. (2020). Winter in two phases: Long-term study of a shallow reservoir in winter. *Limnology and Oceanography*, 1–18. https://doi.org/10.1002/lno.11687

Chorus, I., & Spijkerman, E. (2021). What Colin Reynolds could tell us about nutrient limitation, N : P ratios and eutrophication control. *Hydrobiologia*, *848*(1), 95–111. https://doi.org/10.1007/s10750-020-04377-w

Cole, J. I., & Caraco, N. (1998). Atmospheric exchange of carbon dioxide in a low-wind oligotrophic lake measured by the addition of SF6. *Limnol. Oceanogr.*, *43*(4), 647–656.

Crumpton, W., Isenhart, T., & Mitchell, P. (1992). Nitrate and organic N analyses with second-derivative spectroscopy. *Limnology and Oceanography*, *37*, 907–913.

793 Crusius, J., & Wanninkhof, R. (2003). Gas transfer velocities measured at low wind speed over a lake.
794 *Limnol. Oceanogr.*, *48*, 1010–1017.
795 Davies, J.-M., Nowlin, W. H., & Mazumder, A. (2004). Temporal changes in nitrogen and phosphorus
796 codeficiency of plankton in lakes of coastal and interior British Columbia. *Canadian Journal of*
797 *Fisheries and Aquatic Sciences*, *61*(8), 1538–1551. https://doi.org/10.1139/f04-092
798 DeBeer, C. M., Wheater, H. S., Carey, S. K., & Chun, K. P. (2016). Recent climatic, cryospheric, and
799 hydrological changes over the interior of western Canada: A review and synthesis. *Hydrology*
800 *and Earth System Sciences*, *20*(4), 1573–1598. https://doi.org/10.5194/hess-20-1573-2016
801 Denfeld, B. A., Baulch, H. M., del Giorgio, P. A., Hampton, S. E., & Karlsson, J. (2018). A synthesis of
802 carbon dioxide and methane dynamics during the ice-covered period of northern lakes.
803 *Limnology and Oceanography Letters*, *3*(3), 117–131. https://doi.org/10.1002/lol2.10079
804 Depew, D., Smith, R., & Guildford, S. (2006). Production and respiration in Lake Erie plankton
805 communities. *J. Great Lakes Res.*, *32*, 817–831.
806 Depew, D. C., Guildford, S. J., & Smith, R. E. H. (2006). Nearshore – offshore comparison of chlorophyll a
807 and phytoplankton production in the dreissenid- colonized eastern basin of Lake Erie. *Canadian*
808 *Journal of Fisheries and Aquatic Sciences*, *63*, 1115–1129. https://doi.org/10.1139/F06-016
809 Dokulil, M. T., Herzig, A., Somogyi, B., Vörös, L., Donabaum, K., May, L., & Nõges, T. (2014). Winter
810 conditions in six European shallow lakes: A comparative synopsis. *Estonian Journal of Ecology*,
811 *63*(3), 111–129. https://doi.org/10.3176/eco.2014.3.01
812 D'souza, N. A. (2012). *Psychrophilic diatoms in ice-covered Lake Erie*. Bowling Green State University.
813 Dubourg, P., North, R. L., Hunter, K., Vandergucht, D. M., Abirhire, O., Silsbe, G. M., et al. (2015). Light
814 and nutrient co-limitation of phytoplankton communities in a large reservoir: Lake Diefenbaker,
815 Saskatchewan, Canada. *Journal of Great Lakes Research*, *41*, 129–143.
816 https://doi.org/10.1016/j.jglr.2015.10.001

817 Ducharme-Riel, V., Vachon, D., del Giorgio, P. A., & Prairie, Y. T. (2015). The relative contribution of
818 winter under-ice and summer hypolimnetic CO2 accumulation to the annual CO2 emissions
819 from northern lakes. *Ecosystems*, *18*(4), 547–559. https://doi.org/10.1007/s10021-015-9846-0
820 Edgar, R. E., Morris, P. F., Rozmarynowycz, M. J., D'souza, N. A., Moniruzzaman, M., Bourbonniere, R. A.,
821 et al. (2016). Adaptations to photoautotrophy associated with seasonal ice cover in a large lake
822 revealed by metatranscriptome analysis of a winter diatom bloom. *Journal of Great Lakes*
823 *Research*, (August). https://doi.org/10.1016/j.jglr.2016.07.025
824 Ewing, H., Weathers, K. C., Cottingham, K. L., Leavitt, P. R., Greer, M. L., Carey, C. C., et al. (2020). " New
825 " cyanobacterial blooms are not new : two centuries of lake production are related to ice cover
826 and land use. *Ecosphere*, *11*(June). https://doi.org/10.1002/ecs2.3170
827 Ferrari, I. (1976). Winter limnology of a mountain lake - Lago Santo-Parmense (Northern Appennines,
828 Italy). *Hydrobiologia*, *51*(3), 245–257.
829 Findlay, D. L., & Kling, H. J. (1998). *Protocols for measuring biodiversity: Phytoplankton in freshwater*.
830 Finlay, K., Vogt, R. J., Simpson, G. L., & Leavitt, P. R. (2019). Seasonality of pCO 2 in a hard-water lake of
831 the northern Great Plains: The legacy effects of climate and limnological conditions over 36
832 years. *Limnology and Oceanography*, *64*(January), S118–S129.
833 https://doi.org/10.1002/lno.11113
834 Gammons, C. H., Pape, B. L., Parker, S. R., Poulson, S. R., & Blank, C. E. (2013). Geochemistry, water
835 balance, and stable isotopes of a "clean" pit lake at an abandoned tungsten mine, Montana,
836 USA. *Applied Geochemistry*, *36*, 57–69. https://doi.org/10.1016/j.apgeochem.2013.06.011
837 Gammons, C. H., Henne, W., Poulson, S. R., Parker, S. R., Johnston, T. B., Dore, J. E., & Boyd, E. S. (2014).
838 Stable isotopes track biogeochemical processes under seasonal ice cover in a shallow,
839 productive lake. *Biogeochemistry*, *120*(1–3), 359–379. https://doi.org/10.1007/s10533-014-
840 0005-z

841 Garcia, S. L., Szekely, A. J., Bergvall, C., Schattenhofer, M., & Peura, S. (2019). Decreased snow cover
842 stimulates under-ice primary producers but impairs methanotrophic capacity. *mSphere*, *4*(1).
843 https://doi.org/10.1128/msphere.00626-18
844 Del Giorgio, P. a., & Peters, R. H. (1994). Patterns in planktonic P:R ratios in lakes: Influence of lake
845 trophy and dissolved organic carbon. *Limnology and Oceanography*, *39*(4), 772–787.
846 https://doi.org/10.4319/lo.1994.39.4.0772
847 Glooschenko, W. A., Moore, J. E., Munawar, M., & Vollenweider, R. A. (1974). Primary production in
848 Lakes Ontario and Erie: A comparative study. *J. Fish. Res. Board Can.*, *31*, 253–263.
849 Gosselin, M., Legendre, L., Demers, S., & Ingram, R. G. (1985). Responses of sea-ice microalgae to
850 climatic and fortnightly tidal energy imputs. (Mannitouk Sound, Hudson Bay). *Can. J. Fish. Aquat.*
851 *Sci.*, *42*(Homer 1976), 999–1006. https://doi.org/10.1139/f85-125
852 Grosbois, G., Vachon, D., del Giorgio, P. A., & Rautio, M. (2020). Efficiency of crustacean zooplankton in
853 transferring allochthonous carbon in a boreal lake. *Ecology*, *101*(6).
854 https://doi.org/10.1002/ecy.3013
855 Grosbois, Guillaume, Mariash, H., Schneider, T., & Rautio, M. (2017). Under-ice availability of
856 phytoplankton lipids is key to freshwater zooplankton winter survival. *Scientific Reports*, *7*(1), 1–
857 11. https://doi.org/10.1038/s41598-017-10956-0
858 Guildford, S. J., Depew, D. C., Ozersky, T., Hecky, R. E., & Smith, R. E. H. (2013). Nearshore-offshore
859 differences in planktonic chlorophyll and phytoplankton nutrient status after dreissenid
860 establishment in a large shallow lake. *Inland Waters*, *3*(2), 253–268. https://doi.org/10.5268/iw-
861 3.2.537
862 Guy, R., Berry, J., Fogel, M., & Hoering, T. (1989). Differential fractionation of oxygen isotopes by
863 cyanide-resistant and cyanide-sensitive respiration in plants. *Planta*, *177*, 483–491.

Guy, R., Fogel, M., & Berry, J. (1993). Photosynthetic fractionation of the stable isotopes of oxygen and carbon. *Plant Physiol*, *101*, 37–47.

Hamdan, M., Byström, P., Hotchkiss, E. R., Al-Haidarey, M. J., Ask, J., & Karlsson, J. (2018). Carbon dioxide stimulates lake primary production. *Scientific Reports*, *8*(1), 8–12. https://doi.org/10.1038/s41598-018-29166-3

Hampton, S E, Moore, M. V, Ozersky, T., Stanley, E. H., Polashenski, C. M., & Galloway, A. W. E. (2015). Heating up a cold subject: prospects for under-ice plankton research in lakes. *Journal of Plankton Research*, *37*(2), 277–284. https://doi.org/10.1093/plankt/fbv002

Hampton, Stephanie E., Gray, D. K., Izmest'eva, L. R., Moore, M. V., & Ozersky, T. (2014). The rise and fall of plankton: Long-term changes in the vertical distribution of algae and grazers in Lake Baikal, Siberia. *PLoS ONE*, *9*(2), 1–10. https://doi.org/10.1371/journal.pone.0088920

Hampton, Stephanie E., Galloway, A. W. E., Powers, S. M., Ozersky, T., Woo, K. H., Batt, R. D., et al. (2017). Ecology under lake ice. *Ecology Letters*, *20*(1), 98–111. https://doi.org/10.1111/ele.12699

Hanson, P. C., Bade, D. L., Carpenter, S. R., & Kratz, T. K. (2003). Lake metabolism: Relationships with dissolved organic carbon and phosphorus. *Limnology and Oceanography*, *48*(3), 1112–1119. https://doi.org/10.4319/lo.2003.48.3.1112

Healey, F. P., & Hendzel, L. L. (1979). Fluorometric measurement of alkaline phosphatase activity in algae. *Freshwater Biology*, *9*(5), 429–439. https://doi.org/10.1111/j.1365-2427.1979.tb01527.x

Hecky, R. E., & Guildford, S. J. (1984). Primary productivity of Southern Indian Lake before, during, and after impoundment and Churchill River diversion. *Canadian Journal of Fisheries and Aquatic Sciences*, *41*, 591–604.

Helman, Y., Barkan, E., Eisenstadt, D., Luz, B., & Kaplan, A. (2005). Fractionation of the three stable oxygen isotopes by oxygen-producing and oxygen-consuming reactions in photosynthetic organisms. *Plant Physiol*, *138*, 2292–2298.

Henshaw, T., & Laybourn-Parry, J. (2002). The annual patterns of photosynthesis in two large, freshwater, ultra-oligotrophic Antarctic lakes. *Polar Biology*, *25*(10), 744–752. https://doi.org/10.1007/s00300-002-0402-y

Holmes, R. M., Aminot, A., Kerouel, R., Hooker, B. A., & Peterson, B. J. (1999). A simple and precise method for measuring ammonium in marine and freshwater ecosystems. *Canadian Journal of Fisheries and Aquatic Sciences*, *56*(10), 1801–1808. https://doi.org/10.1139/cjfas-56-10-1801

Howard, D. W., Brentrup, J. A., Richardson, D. C., Lewis, A. S. L., Olsson, F., & Carey, C. C. (2024). Variability in ice cover does not affect annual metabolism estimates in a small eutrophic reservoir. *ESS Open Archive*, (Pre-print). Retrieved from https://essopenarchive.org/doi/full/10.22541/essoar.170689094.45734615

Hrycik, A. R., & Stockwell, J. D. (2020). Under-ice mesocosms reveal the primacy of light but the importance of zooplankton in winter phytoplankton dynamics. *Limnology and Oceanography*, 1–15. https://doi.org/10.1002/lno.11618

Hrycik, A. R., Stockwell, J. D., Rabaey, J. S., Zimmer, K. D., Domine, L. M., Cotner, J. B., et al. (2017). Winter in water: differential responses and the maintenance of biodiversity. *Inland Waters*, *9*(2), 715–725. https://doi.org/10.1016/j.ejrh.2021.100780

Idrizaj, A., Laas, A., Anijalg, U., & Nõges, P. (2016). Horizontal differences in ecosystem metabolism of a large shallow lake. *Journal of Hydrology*, *535*, 93–100. https://doi.org/10.1016/j.jhydrol.2016.01.037

Jähne, B., Münnich, K. O., Bösinger, R., Dutzi, A., Huber, W., & Libner, P. (1987). On the parameters influencing air-water gas exchange. *J. Geophys. Res.*, *92*, 1937–1949.

910 Kalff, J., & Welch, H. E. (1974). Phytoplankton production in Char Lake, a natural polar lake, and in
911 Meretta Lake, a polluted polar lake, Cornwallis-Island, Northwest-Territories. *Journal of the*
912 *Fisheries Research Board of Canada*, *31*(5), 621–636.
913 Katz, S. L., Izmest'eva, L. R., Hampton, S. E., Ozersky, T., Shchapov, K., Moore, M. V, et al. (2015). The
914 "Melosira years" of Lake Baikal: Winter environmental conditions at ice onset predict under-ice
915 algal blooms in spring. *Limnology and Oceanography*, *60*(6), 1950–1964.
916 https://doi.org/10.1002/lno.10143
917 Kiddon, J., Bender, M., Orchardo, J., Caron, D., Goldman, J., & Dennett, M. (1993). Isotopic fractionation
918 of oxygen by respiring marine organisms. *Global Biogeochem Cycles*, *7*, 679–694.
919 Kim, T. Y., North, R. L., Guildford, S. J., Dillon, P., & Smith, R. E. H. (2015). Phytoplankton productivity and
920 size composition in Lake Simcoe: The nearshore shunt and the importance of autumnal
921 production. *Journal of Great Lakes Research*, *41*(4), 1075–1086.
922 https://doi.org/10.1016/j.jglr.2015.09.011
923 Kirk, J. T. O. (1994). *Light and photosynthesis in aquatic ecosystems*. *Light and photosynthesis in aquatic*
924 *ecosystems*. Oxford University Press.
925 Knox, M., Quay, P., & Wilbur, D. (1992). Kinetic isotopic fractionation during air–water gas transfer of O2
926 , N2 , CH4 , and H2. *J Geophys Res*, *97*, 20335–20343.
927 Kroopnick, P., & Craig, H. (1972). Atmospheric oxygen: Isotopic composition and solubility fractionation.
928 *Science*, *175*, 54–55.
929 Lenard, T. (2015). Winter bloom of some motile phytoplankton under ice cover in a mesotrophic lake:
930 vertical distribution and environmental factors. *Oceanological and Hydrobiological Studies*,
931 *44*(2), 164–171. https://doi.org/10.1515/ohs-2015-0016
932 Maeda, O., & Ichimura, S. (1973). On the high density of a phytoplankton population found in a lake
933 under ice. *Internationale Revue Der Gesamten Hydrobiologie*, *5*, 673–689.

McKay, R. M. L., Prášil, O., Pechar, L., Lawrenz, E., Rozmarynowycz, M. J., & Bullerjahn, G. S. (2015). Freshwater ice as habitat: Partitioning of phytoplankton and bacteria between ice and water in central European reservoirs. *Environmental Microbiology Reports*, *7*(6), 887–898. https://doi.org/10.1111/1758-2229.12322

McMeans, B. C., McCann, K. S., Guzzo, M. M., Bartley, T. J., Bieg, C., Blanchfield, P. J., et al. (2017). High-frequency observations of temperature and dissolved oxygen reveal under-ice convection in a large lake. *Inland Waters*, *9*(1), 12,218-12,226. https://doi.org/10.1002/2017GL075373

Noges, T., & Noges, P. (1999). The effect of extreme water level decrease on hydrochemistry and phytoplankton in a shallow eutrophic lake. *Hydrobiologia*, *408*, 277–283.

North, R. L., Barton, D., Crowe, A. S., Dillon, P. J., Dolson, R. M. L., Evans, D. O., et al. (2013). The state of Lake Simcoe (Ontario, Canada): The effects of multiple stressors on phosphorus and oxygen dynamics. *Inland Waters*, *3*(1), 51–74. https://doi.org/10.5268/IW-3.1.529

North, Rebecca L., Johansson, J., Vandergucht, D. M., Doig, L. E., Liber, K., Lindenschmidt, K. E., et al. (2015). Evidence for internal phosphorus loading in a large prairie reservoir (Lake Diefenbaker, Saskatchewan). *Journal of Great Lakes Research*. https://doi.org/10.1016/j.jglr.2015.07.003

North, Rebecca L., Venkiteswaran, J. J., Silsbe, G., Harrison, J. W., Hudson, J. J., Smith, R. E. H., et al. (2023). Year-round metabolism data from Lakes Simcoe (Ontario, 2010-2011), Diefenbaker, Blackstrap, and Broderick (Saskatchewan, 2013-2014), Canada. [Data set]. Environmental Data Initiative. https://doi.org/10.6073/PASTA/AC92E6EB81ACF4B3D6701AA296550DC2

NSIDC: National Snow and Ice Data Center. (2008). U.S. National Ice Center. https://doi.org/10.7265/N52R3PMC

Obertegger, U., Obrador, B., & Flaim, G. (2017). Dissolved oxygen dynamics under ice : three winters of high frequency data from Lake Tovel, Italy. *Water Resources Research*, *53*, 7234–7246.

957 Ontario Ministry of the Environment (OMOE). (2007a). *The determination of ammonia nitrogen and*
958 *nitrate plus nitritie nitrogen in water and precipitation by colourimetry*. (M. of E. L. services
959 branch Quality, Ed.). Toronto, ON, Canada.
960 Ontario Ministry of the Environment (OMOE). (2007b). *The determination of total phosphorus in water*
961 *by colourimetry*. (Ministry of Environment Laboratory services branch quality management, Ed.).
962 Toronto, ON, Canada.
963 Ontario Ministry of the Environment (OMOE). (2008). *The determination of total kjeldahl nitrogen in*
964 *surface water and precipitation by colourimetry*. (Ministry of Environment Laboratory services
965 branch quality, Ed.). Toronto, ON, Canada.
966 Ozersky, T., Bramburger, A., Elgin, A., Vanderploeg, H., Wang, J., Austin, J., et al. (2021). The changing
967 face of winter: Lessons and questions from the Laurentian Great Lakes. *Journal of Geophysical*
968 *Research: Biogeosciences*, *126*, e2021JG006247.
969 Parsons, T. R., Maita, Y., & Lalli, C. M. (1984). *A manual of chemical and biological methods for seawater*
970 *analysis*. Pergamon.
971 Pernica, P., North, R. L., & Baulch, H. M. (2017). In the cold light of day : the potential importance of
972 under-ice convective mixed layers to primary producers. *Inland Waters*, *7*(2), 138–150.
973 https://doi.org/10.1080/20442041.2017.1296627
974 Petty, E. L., Obrecht, D. V., & North, R. L. (2020). Filling in the flyover zone: high phosphorus in
975 Midwestern (USA) reservoirs results in high phytoplankton biomass but not high primary
976 productivity. *Frontiers in Environmental Science*, *8*(111).
977 Powers, S. M., Labou, S. G., Baulch, H. M., Hunt, R. J., Lottig, N. R., Hampton, S. E., & Stanley, E. H.
978 (2017). Ice duration drives winter nitrate accumulation in north temperate lakes. *Limnology and*
979 *Oceanography Letters*, *2*(5), 177–186. https://doi.org/10.1002/lol2.10048

980 Powers, S. M., Baulch, H. M., Hampton, S. E., Labou, S. G., Lottig, N. R., & Stanley, E. H. (2017).
981 Nitrification contributes to winter oxygen depletion in seasonally frozen forested lakes.
982 *Biogeochemistry*. Springer International Publishing. https://doi.org/10.1007/s10533-017-0382-1
983 Quay, P. D., Wilbur, D. O., Richey, J. E., Devol, A. H., Benner, R., & Forsberg, B. R. (1995). The ^{18}O:^{16}O of
984 dissolved oxygen in rivers and lakes in the Amazon Basin: Determining the ratio of respiration to
985 photosynthesis rates in freshwaters. *Limnology and Oceanography*, *40*(4), 718–729.
986 https://doi.org/10.4319/lo.1995.40.4.0718
987 Quinn, C. J., North, R. L., & Dillon, P. J. (2013). Year-round patterns in bacterial production and biomass
988 in Lake Simcoe, Ontario, Canada: are heterotrophic bacteria a significant contributor to low
989 hypolimnetic oxygen? *Inland Waters*, *3*(2), 235–252. https://doi.org/10.5268/iw-3.2.536
990 Rabaey, J. S., Domine, L. M., Zimmer, K. D., & Cotner, J. B. (2021). Winter oxygen regimes in clear and
991 turbid shallow lakes. *JGR Biogeosciences*.
992 Reinl, K. L., Harris, T. D., North, R. L., Almela, P., Berger, S. A., Bizic, M., et al. (2023). Blooms also like it
993 cold. *Limnology and Oceanography Letters*, *8*(4), 546–564. https://doi.org/10.1002/lol2.10316
994 Sadeghian, A., de Boer, D., Hudson, J. J., Wheater, H., & Lindenschmidt, K. E. (2015). Lake Diefenbaker
995 temperature model. *Journal of Great Lakes Research*, *41*, 8–21.
996 https://doi.org/10.1016/j.jglr.2015.10.002
997 Saxton, M. A., D'souza, N. A., Bourbonniere, R. A., McKay, R. M. L., & Wilhelm, S. W. (2012). Seasonal
998 Si:C ratios in Lake Erie diatoms - Evidence of an active winter diatom community. *Journal of*
999 *Great Lakes Research*, *38*(2), 206–211. https://doi.org/10.1016/j.jglr.2012.02.009
1000 Sharma, S., Blagrave, K., Magnuson, J. J., Reilly, C. M. O., Oliver, S., Batt, R. D., et al. (2019). Widespread
1001 loss of lake ice around the Northern Hemisphere in a warming world. *Nature Climate Change*,
1002 *9*(March), 227–231. https://doi.org/10.1038/s41558-018-0393-5
1003 Silsbe, G. M., & Malkin, S. Y. (2015). phytotools: Phytoplankton Production Tools.

1004 Silsbe, Greg M., & Kromkamp, J. C. (2012). Modeling the irradiance dependency of the quantum
1005 efficiency of photosynthesis. *Limnology and Oceanography: Methods*, *10*(9), 645–652.
1006 https://doi.org/10.4319/lom.2012.10.645
1007 Silsbe, Greg. M., Hecky, R. E., & Smith, R. E. H. (2012). Improved estimation of carbon fixation rates from
1008 active flourometry using spectral fluorescence in light-limited environments. *Limnology and*
1009 *Oceanography: Methods*, *10*, 736–751. https://doi.org/10.4319/lom.2012.10.736
1010 Smith, R. E. H., Hiriart-Baer, V. P., Higgins, S. N., Guildford, S. J., & Charlton, M. N. (2005). Planktonic
1011 primary production in the offshore waters of dreissenid-infested Lake Erie in 1997. *J. Great*
1012 *Lakes Res.*, *31*(2), 50–62.
1013 Soetaert, K., Petzoldt, T., & Setzer, R. W. (2010). Solving Differential Equations in R: Package deSolve.
1014 *Journal of Statistical Software*, *33*(9), 1–25.
1015 Solomon, C. T., Bruesewitz, D. A., Richardson, D. C., Rose, K. C., Van de Bogert, M. C., Hanson, P. C., et al.
1016 (2013). Ecosystem respiration: Drivers of daily variability and background respiration in lakes
1017 around the globe. *Limnology and Oceanography*, *58*(3), 849–866.
1018 https://doi.org/10.4319/lo.2013.58.3.0849
1019 Stainton, M. P., Capel, M. J., & Armstrong, F. A. J. (1977). *The Chemical Analysis of Freshwater* (2nd ed.).
1020 Can. Fish. Mar. Serv. Misc. Spec. Publ.,.
1021 Stevens, C., Schultz, D., Vanbaalen, C., & Parker, P. (1975). Oxygen isotope fractionation during
1022 photosynthesis in a blue-green and a green-alga. *Plant Physiol*, *56*, 126–129.
1023 Suarez, E. L., Tiffay, M. C., Kalinkina, N., Tchekryzheva, T., Sharov, A., Tekanova, E., et al. (2019). Diurnal
1024 variation in the convection-driven vertical distribution of phytoplankton under ice and after ice-
1025 off in large Lake Onego (Russia). *Inland Waters*, *9*(2), 193–204.
1026 https://doi.org/10.1080/20442041.2018.1559582

1027 Tassan, S., & Ferrari, G. M. (1995). An alternative approach to absorption measurements of aquatic
1028 particles retained on filters. *Limnology and Oceanography*, *40*(8), 1358–1368.
1029 Twiss, M. R., McKay, R. M. L., Bourbonniere, R. A., Bullerjahn, G. S., Carrick, H. J., Smith, R. E. H., et al.
1030 (2012). Diatoms abound in ice-covered Lake Erie: An investigation of offshore winter limnology
1031 in Lake Erie over the period 2007 to 2010. *Journal of Great Lakes Research*, *38*(1), 18–30.
1032 https://doi.org/10.1016/j.jglr.2011.12.008
1033 Wassenaar, L. I. (2012). Dissolved oxygen status of Lake Winnipeg : Spatio-temporal and isotopic (δ 18 O
1034 – O 2) patterns. *Journal of Great Lakes Research*, *38*, 123–134.
1035 https://doi.org/10.1016/j.jglr.2010.12.011
1036 Webb, D. J., Burnison, B. K., Trimbee, A. M., & Prepas, E. E. (1992). Comparison of chlorophyll a
1037 extractions with ethanol and dimethyl sulfoxide/acetone, and a concern about
1038 spectrophotometric phaeopigment correction. *Canadian Journal of Fisheries and Aquatic*
1039 *Sciences*, *49*(1990), 2331–2336. https://doi.org/10.1139/f92-256
1040 Webb, W. L., Newton, M., & Starr, D. (1974). Carbon dioxide exchange of Alnus rubra. *Oecologia*, *17*,
1041 281–291.
1042 Wetzel, R. G. (1966). Productivity and nutrient relationships in marl lakes of northern Indiana. *Verh. Int.*
1043 *Ver. Limnol.*, *16*, 321–332.
1044 Wetzel, R. G. (2001). Limnology: Lake and River Ecosystems. New York: Academic Press.
1045 Yang, B., Young, J., Brown, L., & Wells, M. (2017). High-Frequency Observations of Temperature and
1046 Dissolved Oxygen Reveal Under-Ice Convection in a Large Lake. *Geophysical Research Letters*,
1047 *44*(24), 12,218-12,226. https://doi.org/10.1002/2017GL075373
1048 Yang, B., Wells, M. G., Li, J., & Young, J. (2020). Mixing, stratification, and plankton under lake-ice during
1049 winter in a large lake: Implications for spring dissolved oxygen levels. *Limnology and*
1050 *Oceanography*, *65*(11), 2713–2729. https://doi.org/10.1002/lno.11543

1051 Yoshida, T., Sekino, T., Genkai-Kato, M., Logacheva, N. P., Bondarenko, N. A., Kawabata, Z.,
1052 Khodzher, T. V., Melnik, N. G., Hino, S., Nozaki, K., Nishimura, Y., Nagata, T., Higashi,
1053 M. and Nakanishi, M. 2003. Seasonal dynamics of primary production in the pelagic zone
1054 of southern Lake Baikal. Limnology. **4**: 53–62. doi:10.1007/s10201-002-0089-3.
1055
1056 Mathias, J. A., and J. Barica. 1980. Factors Controlling Oxygen Depletion in Ice-Covered
1057 Lakes. Can. J. Fish. Aquat. Sci. 37: 185–194. doi:Doi 10.1139/F80-024

Acknowledgements

Funding: Environment Canada's Lake Simcoe Clean-up Fund (LSCUF; REHS, PJD), NSERC (HMB, PJD, SLS, JJH: RGPIN-250060-20), CUPE PDF to RLN, Global Institute for Water Security at the University of Saskatchewan (GIWS; HMB, JJH), Saskatchewan Water Security Agency (JJH: WSA-2012A-0001). The authors declare no conflict of interests.

Technical assistance: L. Aspden, K. Baranowska, D. Bayne, J. Bosch, E. Cavaliere, E. Cvetanovska, P. Dainard, P. Dubourg, R. Elgood, C. English, D. Evans, J. Findeis, B. Ginn, E. Hillis, V. Hiriart-Baer & Environment Canada Technical Operations, C. Hoggart, K. Hunter, B. Johnson, N. Kaur, G. Koehler, V. Kopf, K.E. Lindenschmidt, R. MacLean, S. McInnes, J. Miles, L. Molot, T. Ozersky, C. Quinn, Quinn's Marina, V. Sit, D. Vandergucht, L. Vasko, H. Wilson, D. Weber, S. Xu, H. Yip.